Two-Dimensional NMR Spectroscopy: A Powerful Tool for the Investigation of Molecular Structure and Dynamics

Richard R. Ernst*

Richard R. Ernst: Born 1933 in Winterthur. After his chemistry diploma received at ETH Zürich, he worked from 1958 to 1962 on his PhD thesis at the Laboratorium für Physikalische Chemie under the guidance of Professor Hans Primas. From 1963 to 1968 he was employed by Varian Associates, Palo Alto, California, where he developed NMR Fourier Spectroscopy. Since 1968 he is heading a research group at ETH Zürich working on methodological developments in nuclear magnetic resonance and electron spin resonance, as Privatdozent, Assistant Professor, Associate Professor, and since 1976 as Full Professor. Awards: 1969 Ruzicka Prize, 1983 Gold Medal of the Society of Magnetic Resonance in Medicine, 1985 honory doctor's degree ETH Lausanne, and 1986 Marcel Benoist Prize.

Today chemical research is hardly conceivable without nuclear magnetic resonance. It has proved to be an exceedingly rich source of information for exploring the structure of molecules in solution, for the investigation of solid materials, and for the study of molecular dynamics. In order to cope with the overwhelming information content, an extension to two-dimensional spectroscopy turned out to be indispensibel. Two-dimensional spectroscopy has contributed, since its introduction twelve years ago, a large number of new powerful techniques for the elucidation of coupling networks by 2D correlation spectroscopy, for the measurement of internuclear distances by 2D cross-relaxation spectroscopy, and for the investigation of chemical exchange networks by 2D exchange spectroscopy. These new techniques are particularly useful for the analysis of large molecules in chemistry and in biology.

1. Introduction

The development of nuclear magnetic resonance (NMR) during the past decade has been truely exceptional. Very few fields of chemistry are left that are not yet highly dependent on results obtained by NMR spectroscopy. Moreover, its importance extends nowadays into all fields of natural science from solid state physics to molecular biology[1–3]. Most recently, magnetic resonance has also entered medicine and became a most informative diagnostic tool in clinical applications, both for non-invasive imaging as well as for in-vivo chemical spectroscopy[1,4].

Nuclear spins act like local reporters that provide information on molecular structure in their close vicinity. For chemical applications it is most important that the information is obtained directly in chemical terms. Chemical substituents can readily be identified. Bonding networks as well as bond angles are easily deduced. Even the three-dimensional molecular structure can be determined directly in solution, an achievement which is not matched by any other technique. In addition, NMR spectroscopy is an ideal technique for the study of slow chemical dynamics. A great advantage is that chemical reactions may be studied at leisure in dynamic equilibrium. No fancy stopped flow experiments are needed although they can be combined with NMR if desired.

Much of the recent development has proceeded towards applications for large biomolecules, such as proteins and nucleic acids[2]. It soon turned out that the information content of an NMR spectrum can become overwhelming. And not even the highest conceivable magnetic field strength is sufficient to resolve and identify all spectral features in a conventional one-dimensional NMR spectrum of a biomolecule. Extensions of NMR spectroscopy to more than one dimension seem to be indispensible in order to accommodate the wealth of information in a frequency plane instead on a frequency axis. This calls for two-dimensional (2D) spectroscopy.

Actually, some of the information contained in an NMR spectrum is of truely two-dimensional nature. Consider, for example, the spin-spin couplings for pairs of nuclear spins. In old-fashioned one-dimensional spectroscopy, spin-spin couplings lead to multiplet splittings of the different chemically shifted resonance lines. Sometimes it is easy to identify spins with mutual couplings based on a detailed analysis of the multiplet structure and comparison of the splittings. But the success of such an analysis might be fortuitous. Who knows whether two lines that apparently form together a doublet represent not two independent chemical shifts? This is an unsolvable question when having just a conventional NMR spectrum at hand.

In fact, spin-spin couplings correlate nuclear spins that are near in terms of the chemical bonding network. But correlation information is two-dimensional information and is best represented by a correlation matrix. Rows and columns can be identified with individual spins, and off-diagonal elements indicate couplings between specific nuclei. Such a correlation map can indeed be measured directly as a *2D correlation spectrum* where the diago-

* *Correspondence:* Prof. Dr. R. R. Ernst
Laboratorium für Physikalische Chemie
Eidgenössische Technische Hochschule Zürich
ETH-Zentrum, Universitätstrasse 22
CH-8092 Zürich

nal contains just the conventional one-dimensional spectrum and cross peaks indicate the strength of coupling between nuclear spins at different chemical shift position (cf. Figs. 5, 13, 20, 23).

The situation is very similar for nuclear cross relaxation which presents an invaluable tool for the measurement of internuclear distances for molecules in solution. Cross relaxation relies on magnetic dipole-dipole interaction between spins. It is therefore also a pair interaction that leads to mutual magnetization exchange between spins at different chemical shifts. Again cross relaxation is most naturally represented by a *2D cross-relaxation spectrum* (cf. Fig. 3) where cross peaks measure the rate of magnetization exchange and therefore spatial proximity.

The third phenomenon that also calls for a two-dimensional representation is chemical exchange. Molecular fragments exchange between different chemical environments which are manifested in an NMR spectrum by different chemical shifts. Chemical exchange processes that relate origin and destination of molecular fragments can be visualized in a highly instructive manner by *2D exchange spectroscopy* (cf. Fig. 2). In fact, such a 2D spectrum directly represents the chemical exchange matrix. Both, pathways of exchange and rate constants can be determined in a unique manner.

It may have become apparent that 2D spectroscopy has a very central position in NMR spectroscopy. Indeed it has become an indispensible and powerful tool in many fields of application. Before the experimental techniques of 2D spectroscopy shall be described in detail, three prototype applications will be presented in order to motivate the reader to work also through the more technical Sections 5–13. To acquire some basic knowledge on the modern tools of NMR seems to be a must for most practical chemists.

2. Chemical Exchange Processes Studied by 2D NMR Spectroscopy

It is known that heptamethylbenzenium ion can undergo a dynamic exchange process where methyl groups are moved between the six possible sites[5]. A priori it is unclear whether the dynamics is exclusively due to a 1–2 bond shift as indicated in Fig. 1, or whether intra- or inter-molecular jumps to more remote positions are also feasible. The one-dimensional proton NMR spectrum in Fig. 2, recorded at 40 °C, shows the four chemically inequivalent methyl groups, but it does not reveal an indication of exchange. At higher temperatures, however, severe line broadening, coalescence of the four lines, and line narrowing into a single sharp line occur successively. This behavior can be interpreted in terms of a chemical exchange process. Very careful lineshape studies of one-dimensional spectra in connection with computer simulations led to the conclusion that a 1–2 bond-shift mechanism prevails although the distinction of 1–2 bond-shift and random exchange processes is very difficult[5].

Fig. 2 shows a 2D chemical exchange spectrum of a solution of heptamethylbenzenium ion in 9.4 M H_2SO_4 recorded at 40 °C[6]. The 2D spectrum displays along the marked diagonal four peaks with intensities 2:2:2:1 corresponding to the four types of methyl groups visible also in the 1D spectrum. Three pairs of symmetrically positioned cross peaks, all of equal intensity, indicate exchange exclusively between positions (1, 2), (2, 3), and (3, 4). This confirms immediately and beyond any doubt the predominance of a 1–2 bond-shift mechanism.

The 2D exchange spectrum can be related to the kinetic exchange matrix of the process. The kinetic matrix for a 1–2 bond shift in heptamethylbenzenium ion, formulated in terms of the magnetization of the four magnetically distinct sites, M_1, M_2, M_3, and M_4, can be expressed by the rate constant k for an elementary reaction step between two sites on the Born-Oppenheimer surface:

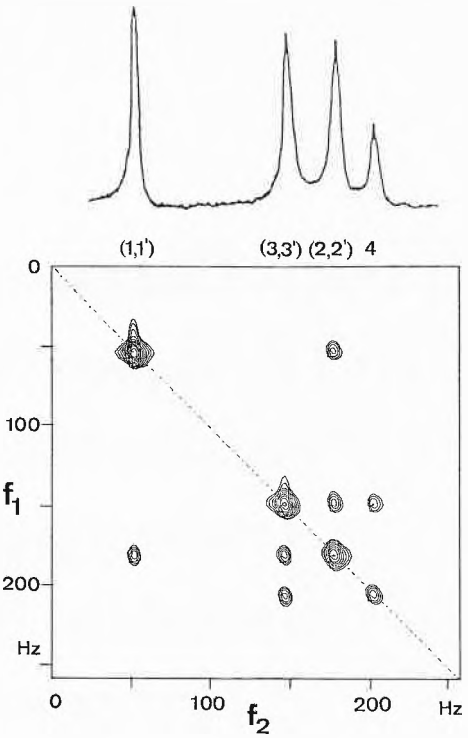

Fig. 2. Contour plot of a 60 MHz proton resonance 2D chemical exchange spectrum of heptamethylbenzenium ion dissolved in 9.4 M H_2SO_4 measured at 40 °C with a mixing time $\tau_m = 280$ ms (adapted from Ref.[6]). A one-dimensional spectrum is shown on top. The assignment of the four peaks is in agreement with Fig. 1.

$$\begin{bmatrix} \dot{M}_1 \\ \dot{M}_3 \\ \dot{M}_2 \\ \dot{M}_4 \end{bmatrix} = \begin{bmatrix} -2k & 0 & 2k & 0 \\ 0 & -4k & 2k & 4k \\ 2k & 2k & -4k & 0 \\ 0 & 2k & 0 & -4k \end{bmatrix} \cdot \begin{bmatrix} M_1 \\ M_3 \\ M_2 \\ M_4 \end{bmatrix} \quad (1)$$

Note that the sites have been ordered according to their appearance in the 2D spectrum. In the initial rate approximation one finds the solution

$$\begin{bmatrix} M_1(t_1, \tau_m) \\ M_3(t_1, \tau_m) \\ M_2(t_1, \tau_m) \\ M_4(t_1, \tau_m) \end{bmatrix} = \begin{bmatrix} 2-4k\tau_m & 0 & 4k\tau_m & 0 \\ 0 & 2-8k\tau_m & 4k\tau_m & 4k\tau_m \\ 4k\tau_m & 4k\tau_m & 2-8k\tau_m & 0 \\ 0 & 4k\tau_m & 0 & 1-4k\tau_m \end{bmatrix} \cdot \begin{bmatrix} f_1(t_1) \\ f_3(t_1) \\ f_2(t_1) \\ f_4(t_1) \end{bmatrix} \cdot M_0 \quad (2)$$

where M_0 is the equilibrium magnetization of a single CH_3 group and $f_1(t_1) \ldots f_4(t_1)$ are modulation functions caused by the evolution during a variable time t_1 that precedes the exchange period and is needed in all 2D experiments as described later. While the matrix in Eq. (1) is asymmetric, the one in Eq. (2) is symmetric. The matrix of Eq. (2)

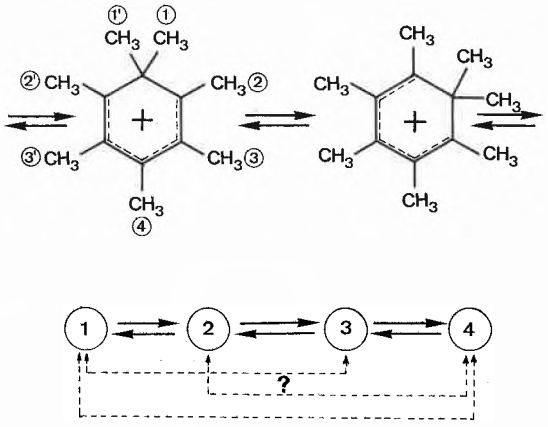

Fig. 1. Chemical exchange processes in heptamethylbenzenium ion. The true chemical exchange network is very complicated and the Born-Oppenheimer surface contains 2520 equivalent minima that differ in the arrangement of the methyl groups. By NMR only four sites, 1, 2, 3, and 4, can be distinguished. In principle, exchange could proceed by a 1–2 bond shift (solid lines) or in addition by random exchange steps (broken lines).

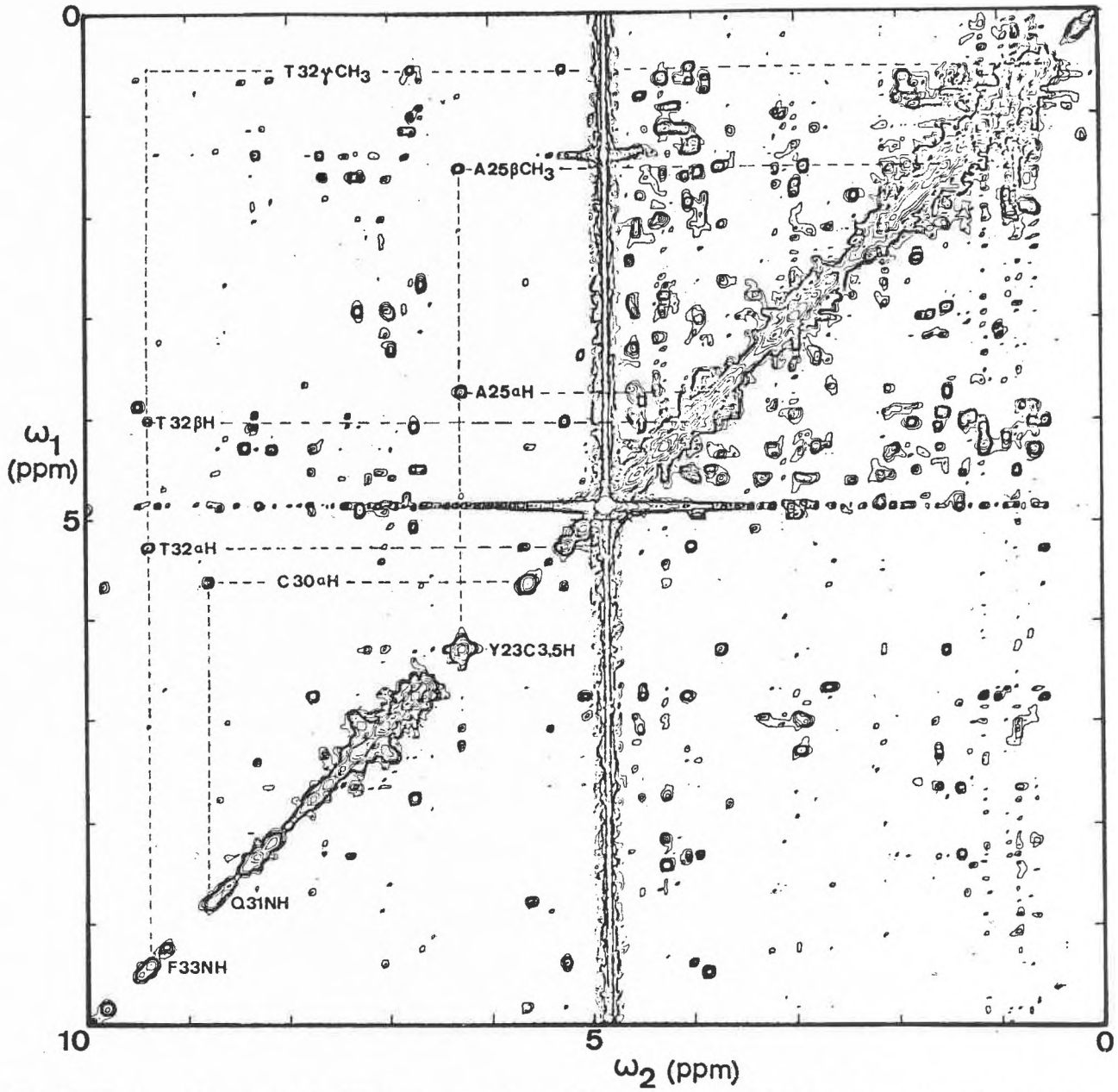

Fig. 3. 360 MHz 2D cross-relaxation (NOESY) spectrum of 20 mM BPTI in ^2H_2O recorded at 18 °C (reproduced from Ref. [9]).

gives directly the intensities of the peaks in the 2D spectrum. Obviously there is close agreement with the experimental spectrum of Fig. 2. All visible off-diagonal peaks have equal intensities, and connect neighbouring sites as expected for 1–2 bond shift. Indeed, it is possible to measure directly the exchange matrix by a simple and straightforward NMR technique.

3. Tertiary Structure of Proteins Determined by 2D NMR Spectroscopy

NMR spectroscopy is in the moment the only technique that allows the determination of the 3D structure of proteins in solution, in contrast to X-ray and neutron scattering which require the sample in single crystalline form. It is known that the crystallization process may alter the tertiary structure and may inhibit motional processes that proceed in solution where the molecules exert their biological function. The solution structure is therefore of first-rate interest. It can be determined by 2D NMR as has been demonstrated first by *Wüthrich* and coworkers [2].

The basic sources of geometric information are the cross-relaxation rates R_{ik} between protons i and k which are induced by magnetic dipole-dipole interactions. They depend on the internuclear distance r_{ik} and on the rotational correlation time τ_c of the molecular tumbling process in solution that modulates the dipole-dipole interaction and causes relaxation according to

$$R_{ik} \propto \tau_c / r_{ik}^6 \qquad (3)$$

Assuming a constant rotational correlation time τ_c throughout the entire molecule, it is possible to estimate distances r_{ik} for nuclear pairs in the molecule from measured cross-relaxation rates R_{ik}.

Cross-relaxation processes can be visualized by 2D cross-relaxation spectroscopy that is usually known under the name 2D nuclear Overhauser effect spectroscopy, abbreviated NOESY. A cross peak between two chemical shift positions indicates cross relaxation between these two sites, the intensity being proportional to the rate constant. The maximum distance r_{ik} for sizeable cross peaks is about 5 Å. Together with constraints imposed by atomic radii and known bond angles, it is then possible to deduce a most likely structure by a sophisticated computer program such as the distance geometry algorithm [7] or by molecular dynamics calculations [8].

Among numerous further biomolecules, the procedure has been applied to the globular protein basic pancreatic trypsin inhibitor (BPTI) with the amino acid sequence RPDFCLEPPYTGGCKARIIRYFYNA KAGLCQTFVYGGCRAKRNNFKSAE DCMRTAGGC, using the one-letter codes for the 58 amino acid residues [2]. A

NOESY spectrum of BPTI is given in Fig. 3. Cross peaks between NH and $C_\alpha H$ protons belonging to adjacent amino acid residues are apparent (e.g. F33NH-T32C_αH, Q31NH-C30C_αH). There are, however, also further proximities among protons of different amino acids more remote in the sequence that lead to strong NOE cross peaks (e.g. Y23$C_{3,5}$H-A25C_αH) and are important for establishing the tertiary structure of the protein.

However, before such a determination of the tertiary structure of a biomolecule can be attempted, it is necessary to arrive at a proper assignment of the backbone protons to the different amino acid residues. Two sources of information are used for the assignment, as illustrated by Fig. 4: (i) NH and $C_\alpha H$ proton pairs within the same amino acid residue are assigned based on their mutual J coupling constant that is revealed in a 2D correlation (COSY) spectrum. Cross peaks arise in a COSY spectrum between two chemical shift positions whenever the two nuclei are related by scalar spin-spin coupling. It is known that all measurable spin-spin couplings are limited to proton pairs within an amino acid residue. (ii) NH and $C_\alpha H$ proton pairs in adjacent amino acid residues can be assigned due to their dipolar cross relaxation which is manifested by cross peaks in a 2D cross-relaxation (NOESY) spectrum. A combination of both spectra permits a step-by-step sequential assignment, often of all backbone protons.

For this sequential assignment of backbone protons, it is convenient to use a triangular combination of a COSY and a NOESY spectrum as shown in Fig. 5. Because of the basic diagonal symmetry of the individual spectra, all relevant information is contained in a triangular cut. The assignment can now proceed sequentially, for example starting with the N24 C_αH-NH COSY cross peak. Cross relaxation between N24NH and Y23C_αH is responsible for a NOESY cross peak that leads to the next residue Y23 where again a NH-C_αH COSY cross peak identifies the NH proton of Y23. This proton exhibits cross relaxation to F22C_αH and leads to a further NOESY cross peak, and so on. The assignment can easily be done by inspection.

As an example for the structure determination of proteins in solution, Fig. 6 shows five backbone structures of another protein, the proteinase inhibitor IIA from bull seminal plasma (BUSI IIA). These structures have been derived by the described procedure and are compatible with the distance constraints obtained from NOESY spectra [11]. Such liquid state structures determined by NMR allow for the first time a comparison with the crystal structures obtained by X-ray scattering.

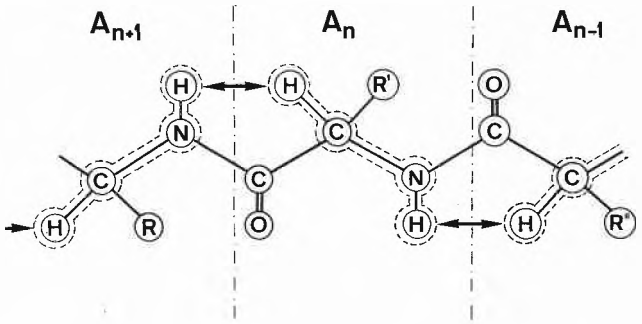

Fig. 4. Nuclear spin coupling network in a polypeptide chain. The broken lines indicate the pathway of the vicinal spin-spin coupling interaction between NH and $C_\alpha H$ protons which is mediated by the electron density and proceeds through the bonds. It is revealed in 2D correlation (COSY) experiments. The arrows indicate through-space magnetic dipolar interaction $\propto 1/r_{ik}^3$ which leads to nuclear cross relaxation with a $1/r_{ik}^6$ distance dependence. It is responsible for cross peaks in NOESY spectra. The two mechanisms of coupling provide a continuous network of interactions extending through the entire polypeptide chain.

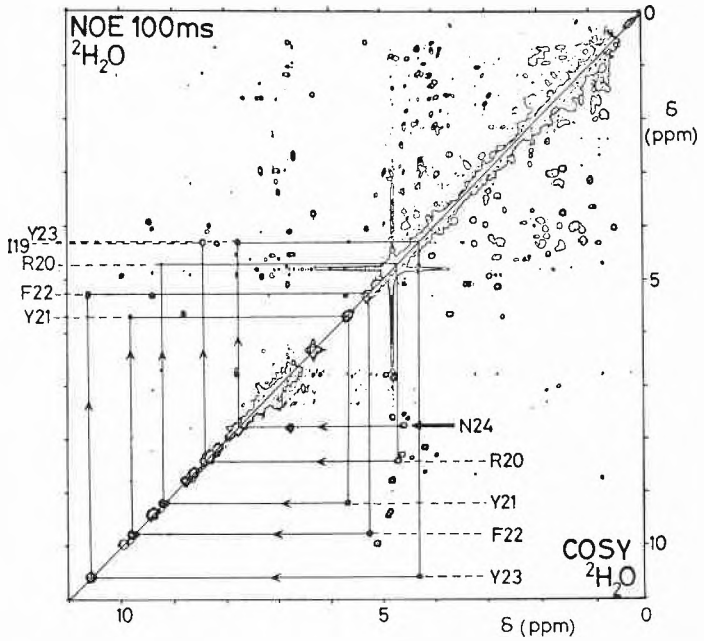

Fig. 5. Triangular combination of a COSY and a NOESY spectrum of BPTI to facilitate the sequential assignment of the backbone protons. J connectivities in the lower half and NOE connectivities in the upper half are indicated by connecting lines starting at the N24 C_αH-NH J cross peak and ending at the R20NH-I19C_αH NOE cross peak. The connectivity «snail» allows unambiguous assignments of the backbone resonance (adapted from Ref. [10]).

4. Heterogeneity of Solid Material Investigated by 2D NMR Spectroscopy

The structure of solid materials can be investigated by NMR spectroscopy based on a phenomenon that is related to cross relaxation in liquids. The dipolar interaction among static protons imbedded in a rigid solid leads to «spin diffusion». When the dipolar coupling between spins is stronger than their chemical shift difference, energy conserving flip-flip processes among the spins are feasible that transfer spin order in a diffusive manner over distances up to 100 Å and more. The spin diffusion rate constant is again proportional to $1/r_{ik}^6$ where r_{ik} is the distance of nearest neighbour spins. It should be noted that spin diffusion in solids is based on a purely static Hamiltonian and describes the evolution of non-equilibrium spin states, while cross relaxation in liquid phase requires rapid molecular motion and is not restricted to spins with similar chemical shifts.

Spin diffusion can be exploited to investigate heterogeneity in solids. Nuclear spins in different, sufficiently large domains do not cross-talk while spins in the same domain may take part in spin diffusion. A 2D experiment analogous to 2D exchange spectroscopy in liquids allows one to visualize spin diffusion. Cross peaks between the resonances of two spins in a spin diffusion spectrum indicate then spatial proximity in a solid.

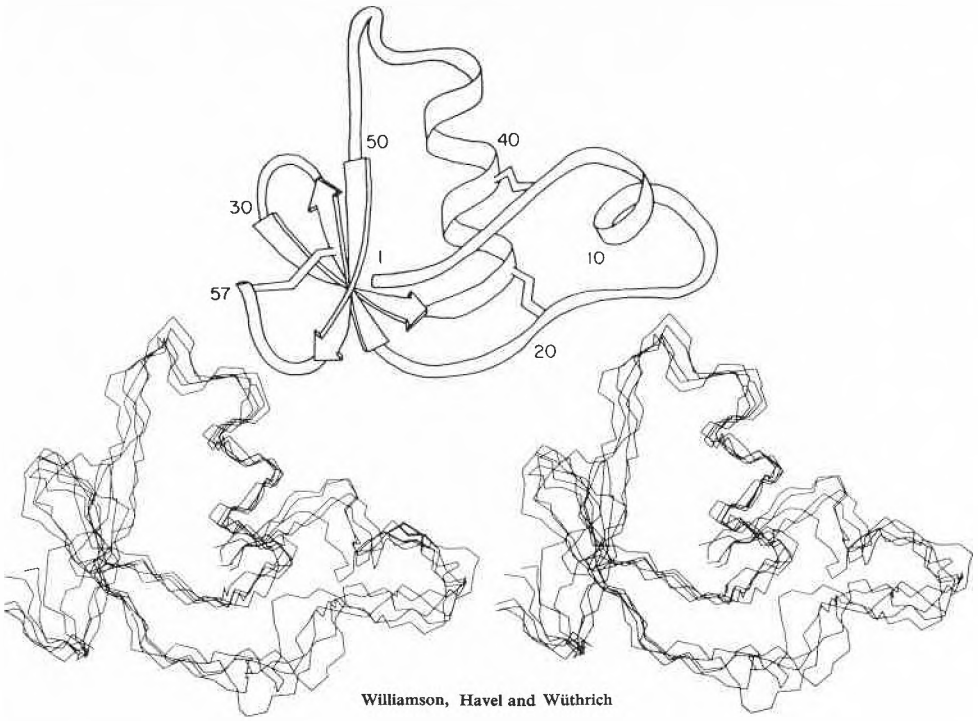

Fig. 6. Stereographic views of 5 computer-optimized backbone structures of BUSI IIA based on distance constraints derived from NOESY spectra. The first 4 residues and the disulfide bonds have been omitted for clarity. In addition, a schematic drawing of the backbone structure is included (reproduced from Ref. [11]*).*

The utility of spin diffusion shall be illustrated by an investigation of polymer blends obtained by casting the blends from a solution of two or more polymers in a suitable solvent. It is known that the physical properties of polymer blends depend on the heterogeneous or homogeneous domain structure of the blend. It is also known that the micro structure can be affected by the solvent and by the casting procedure.

Fig. 7 shows the solid state one-dimensional proton NMR spectra of two blends of polystyrene and polyvinylmethylether cast by adding petroleum ether to a solution either in toluene (blend B_T) or in chloroform (blend B_C)[12]. The spectra differ only very slightly and do not allow conclusions on heterogeneity.

2D spin diffusion spectra of the two blends are presented in Fig. 8. The aromatic proton peak is characteristic for polystyrene while the OCH_3, OCH peak arises from polyvinylmethylether. Spin diffusion between these two peaks provides the required information. Indeed the two 2D spectra differ significantly. The 2D spectrum for the blend B_C shows no cross peaks between the mentioned resonances and must be fully heterogeneous. There seems to be no mixed domain containing the two polymers. The 2D spectrum for the blend B_T, on the other hand, exhibits strong cross peaks between the resonances of different polymers. It contains therefore a homogeneous domain in which the two polymers are mixed on a molecular scale.

It has turned out[13] that the exact composition of the various domains cannot be determined based on a 2D spin diffusion spectrum alone. However, in combination with selective saturation experiments, it proved possible to obtain the composition of blend B_T in terms of a simple three-phase model[12]. The pure polystyrene phase contains 8%, the mixed phase 79%, and the pure polyvinylmethylether phase 13% of the total polymer mass. The mixed phase consists to 63% of polystyrene.

Although the experiment is conceptually very simple and the resulting spectra easy to interprete, the experimental requirements for solids are more stringent than in solution. Magic angle sample spinning and multiple pulse dipolar decoupling are needed in order to obtain sufficient spectral resolution.

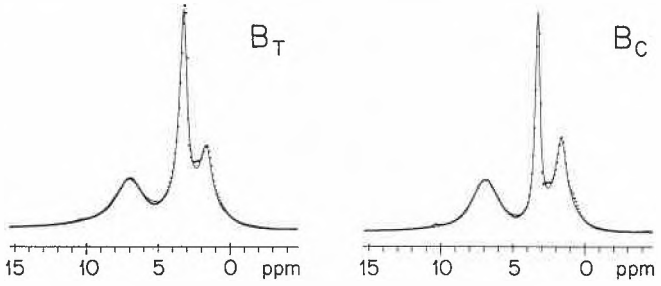

Fig. 7. Solid state proton resonance spectra of two polymer blends. B_T: blend consisting of 44 mol% polystyrene and 56 mol% polyvinylmethylether cast from toluene; B_C: blend consisting of 53 mol% polystyrene and 47 mol% polyvinylmethylether cast from chloroform. The dots represent the experimental signal, the solid lines indicate a computer fit from which the concentrations were determined. Multiple pulse dipolar decoupling by MREV-8 and magic angle sample spinning were employed to enhance resolution (reproduced from Ref. [12]*).*

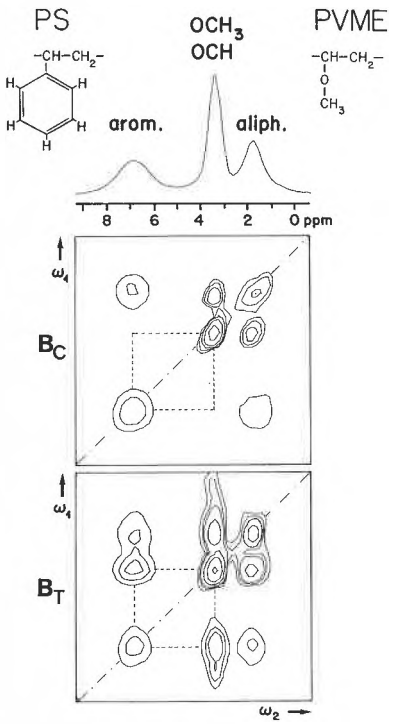

Fig. 8. 2D spin diffusion spectra of the two polymer blends B_T and B_C obtained with the experimental scheme of Fig. 11. The position of expected cross peaks between aromatic protons of polystyrene (PS) and the OCH_3 and OCH protons of polyvinylmethylether (PVME) are marked by broken lines (adapted from Ref. [13]*).*

5. The Basic 2D Experiments

The 2D spectra described so far have been obtained by the same basic experimental scheme, shown in Fig. 9: A signal $s(t_1, t_2)$ is measured as a function of the real time variable t_2, while the time parameter t_1 is incremented from experiment to experiment in a extended series of measurements. The two-dimensional time domain signal

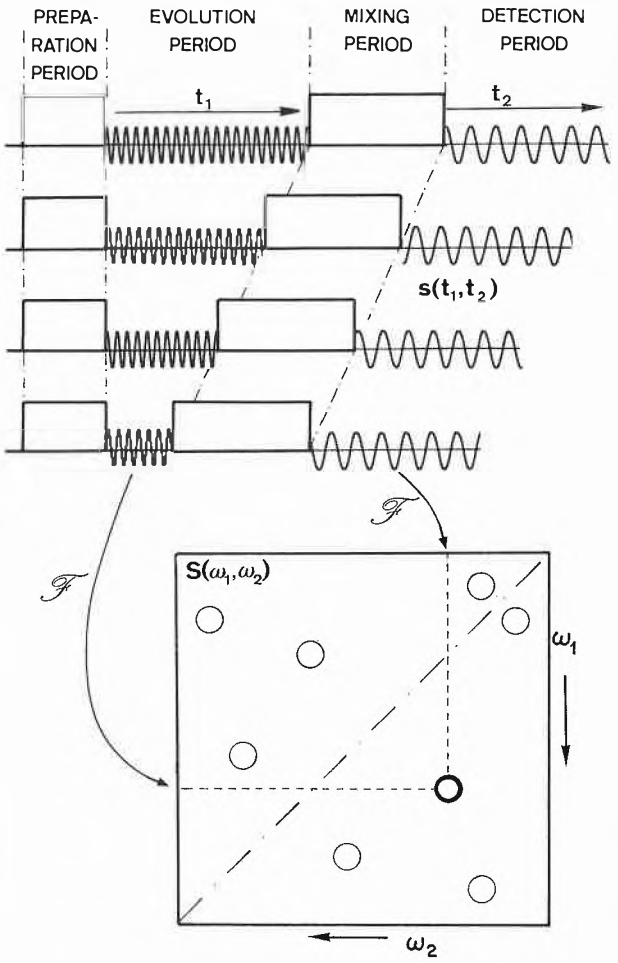

Fig. 9. Schematic representation of a 2D experiment consisting of four periods: preparation, evolution, mixing, and detection. The evolution period t_1 is varied systematically in duration in a series of experiments. The signal $s(t_1, t_2)$ is measured in the detection period as a function of t_2. The precession during the evolution period causes an oscillatory dependence on t_1 of the initial signal amplitude $s(t_1, 0)$. A two-dimensional Fourier transformation delivers the 2D spectrum shown at the bottom. It can be perceived as a representation of the mixing process that transfers coherence between different transitions.

$s(t_1, t_2)$ is then Fourier-transformed in two dimensions and leads to the 2D spectrum $S(\omega_1, \omega_2)$. This type of time-domain Fourier-transform spectroscopy is the most frequently used approach to 2D spectroscopy although further procedures are conceivable[1]. It is for example possible to compute 2D spectra from the stochastic response of non-linear systems[14].

The notion «coherence» is of central importance in 2D spectroscopy[1]. It denotes the in-phase motion of an ensemble of particles, in our case of spin magnetic moments. This is in contrast to motion of spins with random phases. Coherence is induced by radio frequency (rf) pulses and its components can be attributed to individual transitions between levels in an energy level scheme that proceed in a coherent manner. Sometimes, coherence can be associated with precessing transverse magnetization of a particular spin I_k. In this case, it may be represented symbolically by one of the transverse spin operators I_{kx} or I_{ky}, depending on its phase. (The z axis is the direction of the external static magnetic field.) In the presence of an additional spin I_l with spin quantum number $I_l = 1/2$, one may also speak of «anti-phase coherence», or more specifically of coherence of spin I_k anti-phase with respect to spin I_l. This implies that the amplitude of coherence of spin I_k has a sign that depends on the sign of polarization of spin I_l with respect to the external field. Anti-phase coherence may symbolically be represented by the operators $I_{kx}I_{lz}$ and $I_{ky}I_{lz}$ [1, 15] or more losely visualized by antiparallel transverse vectors belonging to the two I_k transitions with different I_l polarization. This operator description, although useful, will no extensively be applied in the following.

The basic four-phase time-domain experiment, sketched in Fig. 9, starts with the *preparation period* that serves to excite coherence. Numerous excitation processes are conceivable. In the simplest case a non-selective $\pi/2$ pulse is used as in Figs. 10a–10d, which can be extended into a sequence of several pulses, for example to excite multiple quantum transitions (Fig. 10e) or in order to transfer polarization to another less sensitive spin species (see Fig. 25).

The purpose of the *evolution period* is to determine the characteristic resonance frequencies of the molecules before the transfer of coherence by pulses, chemical exchange, or cross relaxation. The evolution during this period is responsible for the frequency spread of the 2D spectrum in the ω_1 direction. It may take place under the natural Hamiltonian or under an effective Hamiltonian caused by a suitable rf perturbation, such as a central refocusing π pulse or a spin decoupling sequence. We may understand the function of the evolution period that precedes the mixing or exchange period by visualizing that the individual spins are «labeled» with their precession frequencies measured during the evolution period in order to determine their origin after the mixing or exchange process.

The following *mixing period* is in many experiments the most important period. It serves to effect the coherence transfer that is mapped in the form of a 2D spectrum. Coherence transfer can be induced by an unitary transformation caused by a series of rf pulses (cf. Fig. 10a, 10c, 10e). On the other hand it is also possible to initiate an incoherent transfer process that transfers coherence («coherence» can in fact be transferred incoherently!) by chemical exchange, cross relaxation, or by spin diffusion (Fig. 10b and Fig. 11). In some 2D experiments, designed for 2D separation, the mixing period may be absent altogether.

In the final *detection period*, the coherence resulting from the coherence transfer process is detected and recorded. Again it is possible to let proceed the evolution during detection under a suitably modified Hamiltonian.

A principal and general characteristic of time-domain 2D experiments is the mode of recording. The observation of the signal $s(t_1, t_2)$ is strictly limited to the detection period t_2. The information on evolution during the evolution period t_1 is obtained indirectly by systematic incrementation of the evolution time t_1 in an extended series of experiments that delivers the 2D data set $s(t_1, t_2)$. The 2D array of time-domain data is then subjected to a 2D Fourier transformation producing the 2D spectrum $S(\omega_1, \omega_2)$. This recording procedure is responsible for the often considerable performance time of 2D experiments requiring frequently several thousand individual experiments for different t_1 values. Usually no reduction in performance time is possible because the amount of information inherent in the 2D spectrum $S(\omega_1, \omega_2)$ must be matched by the data acquisition process. Nevertheless time-saving tricks are known that are applicable in special situations.

It should have become clear that an almost unlimited multitude of 2D techniques is conceivable of which many are already of practical importance. The basic principle is quite general and can be applied to all

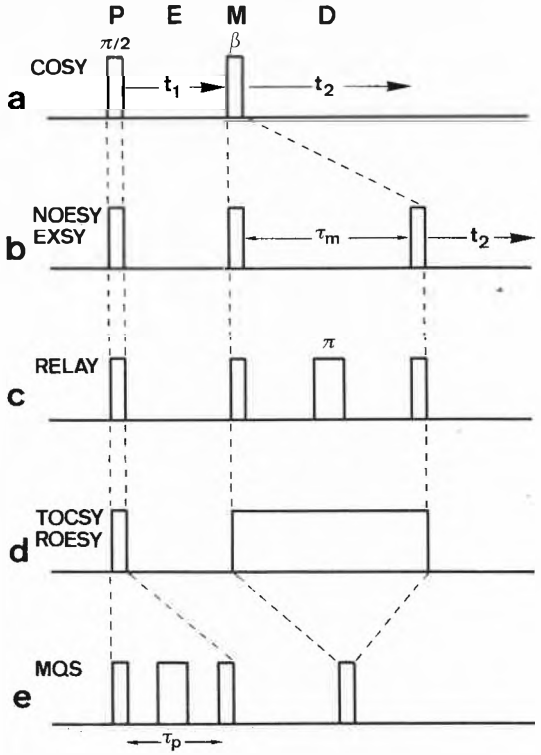

Fig. 10. A collection of some important 2D experiment pulse sequences. The four relevant periods are denoted P = preparation, E = evolution, M = mixing, and D = detection. – (a) Homonuclear 2D correlation spectroscopy (COSY) with a single π/2 preparation and a single mixing pulse of rotation angle β. – (b) 2D exchange spectroscopy for the investigation of chemical exchange (EXSY) or for cross relaxation (NOESY). During the mixing period z magnetization is exchanged between different sites. Two π/2 pulses are needed to rotate magnetization from the transverse plane to the z axis and vice versa. – (c) 2D relayed correlation spectroscopy (RELAY COSY). The mixing period involves a two-step coherence transfer effected by two π/2 pulses. The central π pulse serves to refocus chemical shift precession. Note the similarity to the NOESY experiment of (b). Different coherence transfer pathways are selected in the two experiments by phase cycling. – (d) Total correlation spectroscopy (TOCSY) and rotating frame NOE spectroscopy (ROESY). The transfer of coherence takes place in the presence of an extended period of rf irradation («in the rotating frame»). – (e) 2D multiple quantum spectroscopy. The initial creation of multiple quantum coherence requires a three-pulse preparation sequence. A single mixing pulse converts non-detectable multiple quantum coherence into observable single quantum coherence.

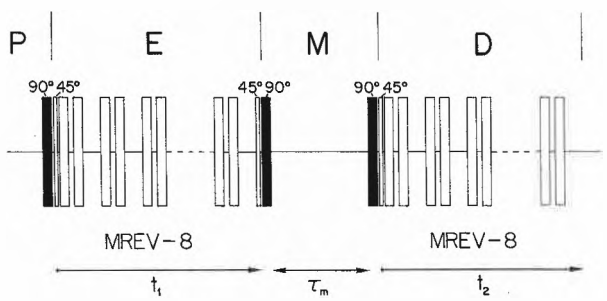

Fig. 11. Experimental pulse scheme for 2D proton spin diffusion measurements. The π/2 preparation pulse is followed by a MREV-8 multiple pulse dipolar decoupling sequence applied during the evolution period bracketed by two 45° pulses needed in order to rotate the magnetization to and from the average quantization axis. The same procedure is applied during the detection period. During the mixing period, no decoupling is applied in order to allow for spin diffusion. Magic angle sample spinning (not shown) is used throughout the entire experiment to eliminate chemical shielding anisotropy (reproduced from Ref. [13]).

fields of spectroscopy although practical difficulties outside of NMR might be severe. So far, most 2D experiments have been performed in NMR together with a few experiments in nuclear quadrupole resonance and in electron spin resonance.

The 2D spectroscopy techniques can be grouped in three classes:

(i) Experiments of 2D separation. This class comprises techniques that do not require a mixing period and effect a 2D spread of a 1D spectrum by evolution under two different effective Hamiltonians. Unlike 2D correlation, the number of peaks in the 2D separated spectrum is identical to the number of resonances in the 1D spectrum. Proton and carbon-13 2D *J* spectra of liquid samples as well as separated local field spectra of solids belong to this category [1]. Experiments of this type will not be covered by this essay.

(ii) Experiments of 2D correlation. The coherence transfer during mixing is caused by an unitary transformation induced by rf pulses. This experiment serves for the investigation of connectivity through *J* coupling and possibly through dipolar interaction. The simple pulse scheme of the prototype experiment for homonuclear 2D correlation spectroscopy, first proposed by *Jeener* [16], is shown in Fig. 10a. It uses a $\pi/2$ preparation pulse that excites all allowed single quantum coherences. The coherence transfer in the mixing period is effected by a single $\pi/2$ pulse which transfers coherence exclusively between transitions of spins that are scalar coupled.

Coherence transfer is restricted to anti-phase coherence, such as $I_{kx}I_{lz}$. A $(\pi/2)_y$ mixing pulse causes the transformation [15]

$$I_{kx}I_{lz} \xrightarrow{(\pi/2)_y} -I_{kz}I_{lx} \qquad (4)$$

Coherence of spin I_k anti-phase with respect to spin I_l is thereby transferred into coherence of spin I_l anti-phase with respect to spin I_k. This is the basic transfer process in pulsed coherence transfer. It leads to an anti-phase square cross-peak multiplet pattern with positive and negative intensities in the arrangement $[\pm \mp]$ which is the basic structure element of all cross peaks in 2D correlation spectroscopy. It is visible in the schematic Fig. 18 and in the experimental Figs. 16, 19, 20, 23. Further examples are heteronuclear 2D correlation spectroscopy (Fig. 25), 2D relayed correlation spectroscopy (Fig. 10c), total correlation spectroscopy (TOCSY, Fig. 10d), and 2D multiple quantum spectroscopy (Fig. 10e).

(iii) 2D exchange experiments. The transfer of spin order during mixing is effected by an incoherent process. The goal of this class of experiments is the investigation of processes such as chemical exchange, cross relaxation, and spin diffusion in the laboratory or in the rotating frame (Fig. 10b and Fig. 10d).

The 2D exchange experiment used for Fig. 2 employs the pulse scheme of Fig. 10b. After evolution for a time t_1, a $\pi/2$ pulse re-establishes z magnetization that depends in an oscillatory manner on t_1. In the course of the mixing time τ_m chemical exchange may take place. The second $\pi/2$ mixing pulse is used for sampling magnetization that exchanged or that remained on the original site.

The same pulse sequence is also used for 2D cross-relaxation spectroscopy (NOESY), an example of which is shown in Fig. 3. Regarding NMR phenomena, it is immaterial whether magnetization is exchanged by chemical exchange or by cross relaxation.

Another application of the 2D exchange pulse sequence is the measurement of proton spin diffusion as exemplified in Fig. 8. The detailed pulse scheme, shown in Fig. 11, has however to take account of two complications: In order to obtain sufficient spectral resolution to distinguish the inequivalent protons it is necessary to eliminate the dipolar interactions during evolution and detection periods. For this purpose one of the well-known multiple pulse dipolar decoupling pulse sequences is applied, such as the MREV-8 sequence. In addition it is also necessary to rotate with about 3 kHz the sample about the magic angle axis to suppress the chemical shielding anisotropy which would otherwise also ruin resolution[12]. These refinements are required for the resolution shown in Figs. 7 and 8.

It should be noted that the extremely successful NMR imaging experiments used in magnetic resonance (MR) tomography for medical diagnosis are predominantly based on the very same principles[4]. In particular the Fourier imaging method is intimately related to 2D spectroscopy[1, 17].

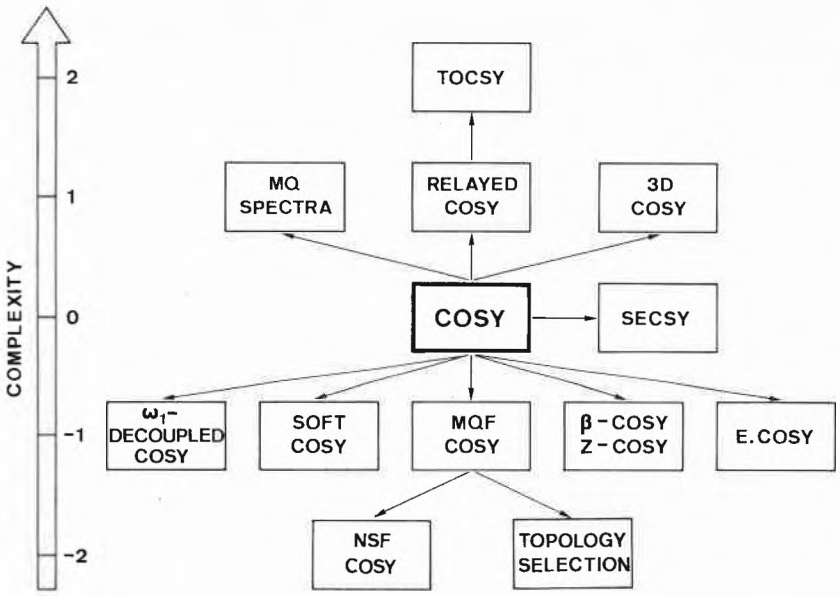

Fig. 12. Hierachical tree of 2D correlation techniques. The various methods are grouped according to the degree of complexity of the resulting 2D spectra.

6. Extensions of 2D Correlation Spectroscopy

Numerous useful extensions of the basic 2D experiments have been proposed. We concentrate in the following on the rich family of 2D correlation techniques. The hierarchical tree of techniques is given in Fig. 12 with various members grouped according to the degree of complexity of the resulting 2D spectra in terms of the number of possible cross peaks.

On complexity level "0" is the primordial ancestor, 2D correlation spectroscopy COSY, and also 2D spin echo correlated spectroscopy (SECSY)[1] that differs exclusively in the spatial arrangement of the peaks in the 2D frequency plane and requires in favourable cases fewer experimental scans to be performed.

The techniques on complexity level "1" produce cross peaks also among next nearest neighbours within the scalar coupling network, displayed either in two dimensions by relayed COSY and 2D multiple quantum spectroscopy, or in three dimensions by 3D COSY. The maximum number of cross peaks can be obtained by total correlation spectroscopy (TOCSY or HOHAHA) on complexity level "2".

On the other hand, various means for simplifying 2D spectra by restricting coherence transfer have been proposed. On complexity level "−1" one finds techniques that select coherence transfer according to an intermediate multiple quantum coherence stage (MQF COSY) or according to connectivity of transitions in the energy level diagram (E.COSY, β-COSY, z-COSY). Spin decoupling (ω_1-decoupled COSY) and selective excitation (soft-COSY) are additional means of simplification. Further reduction of the number of cross peaks can be attained on complexity level "−2" by selecting spin systems with a predetermined number of spins (NSF COSY) or with a specific topology of the spin coupling network (topology selection).

Some of these possibilities will be illustrated in the following.

7. Relayed Correlation Spectroscopy

In a conventional 2D correlation (COSY) spectrum cross peaks occur exclusively between nearest neighbours in a spin coupling network. In the case of incomplete spectral resolution, this might sometimes lead to ambiguities in the assignment of resonances. They may be resolved when also two-step relayed coherence transfers, relating next nearest neighbours, are made allowed.

It is easy to conceive a suitable technique for this purpose[18]. Instead of a single mixing pulse as in Fig. 10a, two mixing pulses are needed, leading to the scheme of Fig. 10c. Chemical shielding precession is undesired during the mixing period τ_m and is refocused by a π pulse applied at the center of the mixing period.

The two-step relayed coherence transfer can conveniently be followed in terms of product operators representing the actual state of the system (density operator). Let us assume a linear three-spin coupling network of the type

$$I_k \overset{J_{kl}}{—} I_l \overset{J_{lm}}{—} I_m \qquad (5)$$

with the two scalar coupling constants J_{kl} and J_{lm}. The transfer of I_k coherence to spin I_m proceeds as follows (disregarding chemical shift precession)[15]

$$I_{kz} \xrightarrow{(\pi/2)I_{ky}} I_{kx} \xrightarrow{(\pi J_{kl}t_1)2I_{kz}I_{lz}} 2I_{ky}I_{lz}$$

$$\xrightarrow{(\pi/2)(I_{kx}+I_{lx})} -2I_{kz}I_{ly}$$

$$\xrightarrow{(\pi J_{kl}\tau_m)2I_{kz}I_{lz}+(\pi J_{lm}\tau_m)2I_{lz}I_{mz}} 2I_{ly}I_{mz}$$

$$\xrightarrow{(\pi/2)(I_{lx}+I_{mx})} -2I_{lz}I_{my} \qquad (6)$$

The single operators above the arrows indicate $\pi/2$ rotations of the corresponding spin about the indicated axis. The operator products above the arrows, on the other hand, represent (bilinear) transformations induced by the J couplings whereby it has been assumed that $(\pi J_{kl}t_1) = \pi/2$ and $(\pi J_{kl}\tau_m) = (\pi J_{lm}\tau_m) = \pi/2$. The latter rela-

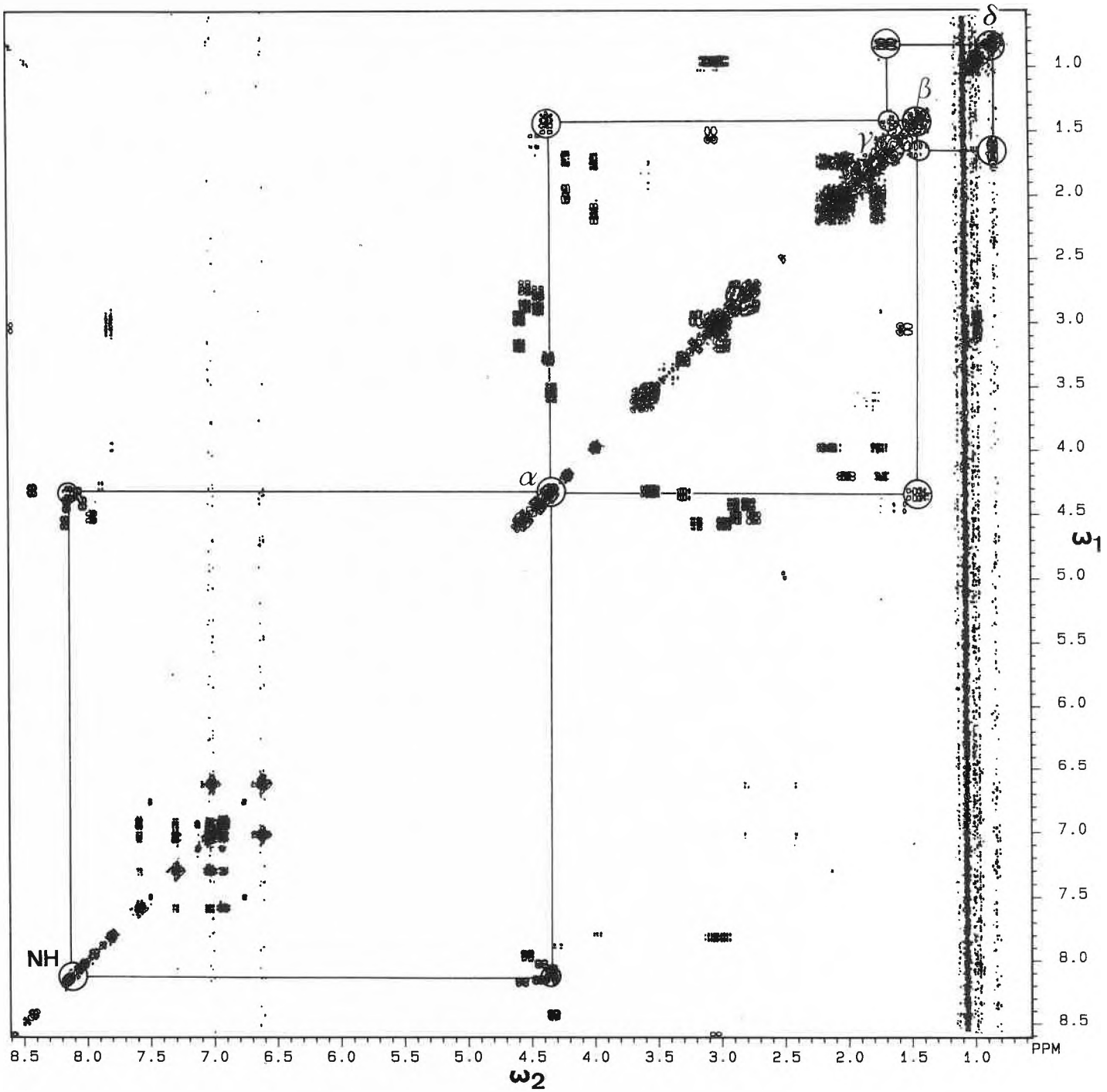

Fig. 13. 300 MHz proton resonance double quantum-filtered COSY spectrum of the nonapeptide buserilin dissolved in dimethyl sulfoxide. The pulse sequence of Fig. 17 was used. A phase-sensitive plot with equal representation of positive and negative contours is shown. The resonance connectivities of leucine are indicated [19].

tion leads to maximum transfer efficiency and puts a condition on the selection of the mixing time τ_m. It can be fulfilled exactly only for equal couplings $J_{kl} = J_{lm}$. This shows that relayed coherence transfer requires a delicate compromise in the selection of τ_m, and transfer will in practice often be far from optimum for many relayed correlation peaks in a spectrum.

Relayed coherence transfer will be demonstrated with 300 MHz proton spectra of the linear nonapeptide buserilin, pyro-Glu-His-Trp-Ser-Tyr-D-Ser-Leu-Arg-Pro-$NHCH_2CH_3$ (p-E-H-W-S-Y-S-L-R-P-NHEt). Fig. 13 shows the COSY spectrum and Fig. 14 a relayed COSY spectrum [19]. In both spectra the resonance connectivities of the residue leucine are marked. It is seen that in COSY only nearest neighbour cross peaks occur: NH-C_αH, C_αH-$C_\beta H_{1,2}$, $C_\beta H_{1,2}$-C_γH, and C_γH-C_δH. On the other hand, in the relayed COSY spectrum also the next nearest neighbour cross peaks NH-$C_\beta H_{1,2}$ and $C_\beta H_{1,2}$-C_δH occur. The third pair of relayed cross peaks $C_\alpha H$–$C_\gamma H$ is weak due to the high multiplicity of the C_γH resonance and not visible in the contour representation of Fig. 14.

8. 2D Spectroscopy in the Rotating Frame

Having achieved coherence transfer over two steps, it is easy to generalize the experiment to an arbitrary number of transfer steps. It is just necessary to expand the mixing sequence of Fig. 10c to a large number of mixing pulses. In the end, virtually a continuous rf irradiation for the time τ_m is obtained as indicated in Fig. 10d. This experiment leads to coherence transfer throughout the entire coupled spin system, limited only by relaxation decay of the coherence [20]. This experiment is called

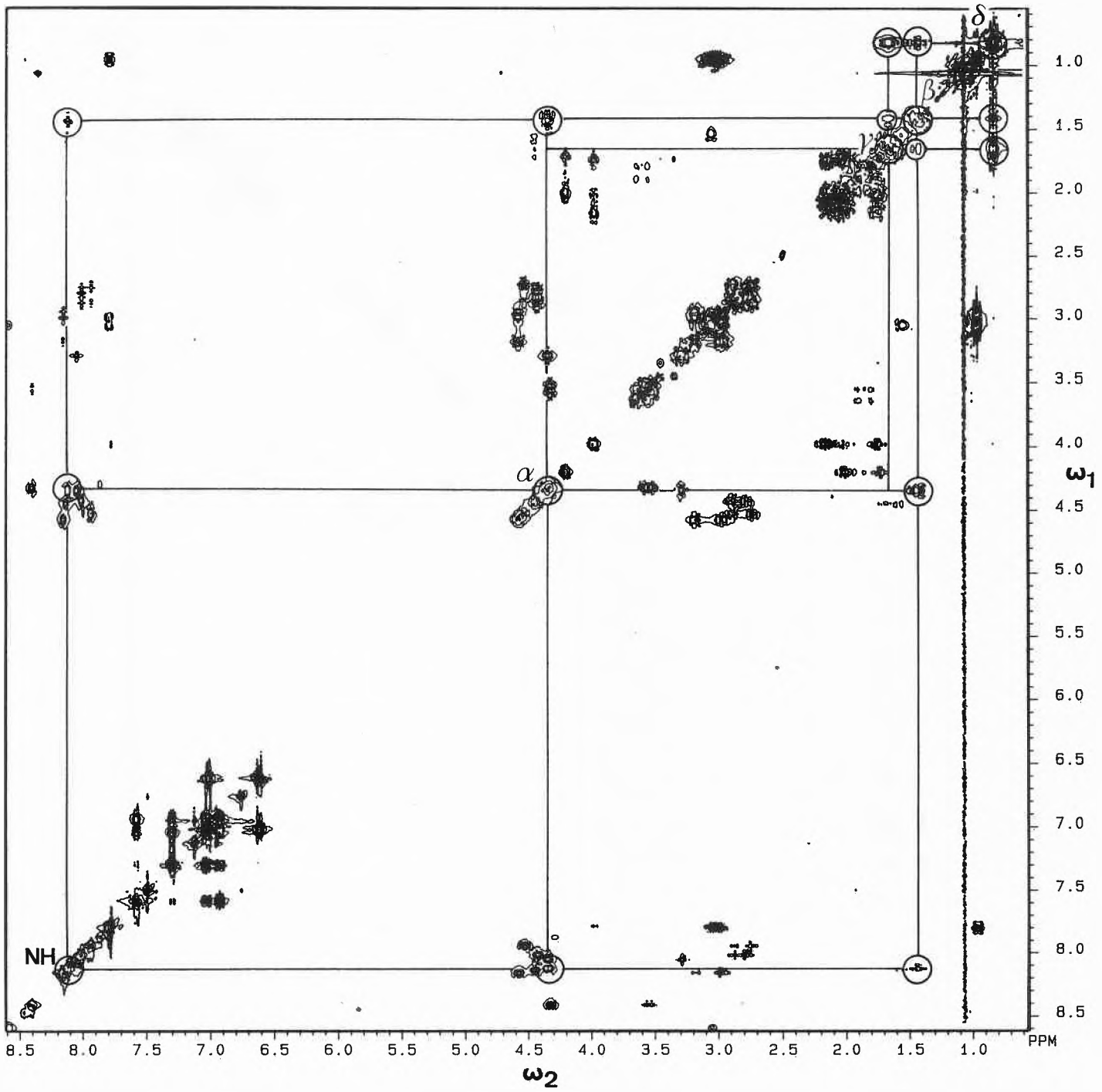

Fig. 14. 300 MHz relayed COSY spectrum of the nonapeptide buserilin dissolved in dimethyl sulfoxide. The pulse sequence of Fig. 10c was applied with a mixing time τ_m = 25 ms. A phase-sensitive plot with equal representation of positive and negative contours is shown. The resonance connectivities of leucine are indicated [19].

total correlation spectroscopy (TOCSY) [20] or homonuclear Hartmann-Hahn (HOHAHA) spectroscopy [21].

The latter term puts the experiment in connection with Hartmann-Hahn cross polarization in the rotating frame [22] and with spin diffusion as explained in Section 4. The evolution of the spin system can be conceived in a frame rotating with the applied rf field. In the resulting time-independent rotating-frame Hamiltonian, the chemical shift differences are effectively quenched and energy conserving flip-flop processes of the spins connected by scalar couplings become feasible. This leads to spin diffusion processes that are limited only by the extensions of the coupling network. The efficiency of the chemical shift quenching over a large spectral range can be enhanced by the application of more sophisticated pulse sequences [21].

Fig. 15 gives a TOCSY spectrum of buserilin that can be compared with the COSY and relayed COSY spectra of Fig. 13 and Fig. 14, respectively [19]. Again the resonance connectivities for leucine are marked. Here also three-step transfers $C_\alpha H$-$C_\delta H$ and even four-step transfers NH-$C_\delta H$ are visible. Again some expected cross peaks involving $C_\gamma H$ are missing because of the extensive multiplet structure of $C_\gamma H$. Similar features are also apparent for other residues.

It should be mentioned that in addition to the coherent transfer through *J* coupling also incoherent transfer of magnetization through cross relaxation can occur under the application of an rf field during mixing. This leads to additional cross peaks that are analogous to NOESY cross peaks. Cross relaxation in the rotating frame has favourable properties in comparison to laboratory frame cross relaxation. For molecules of intermediate size, the laboratory frame cross-relaxation rate changes

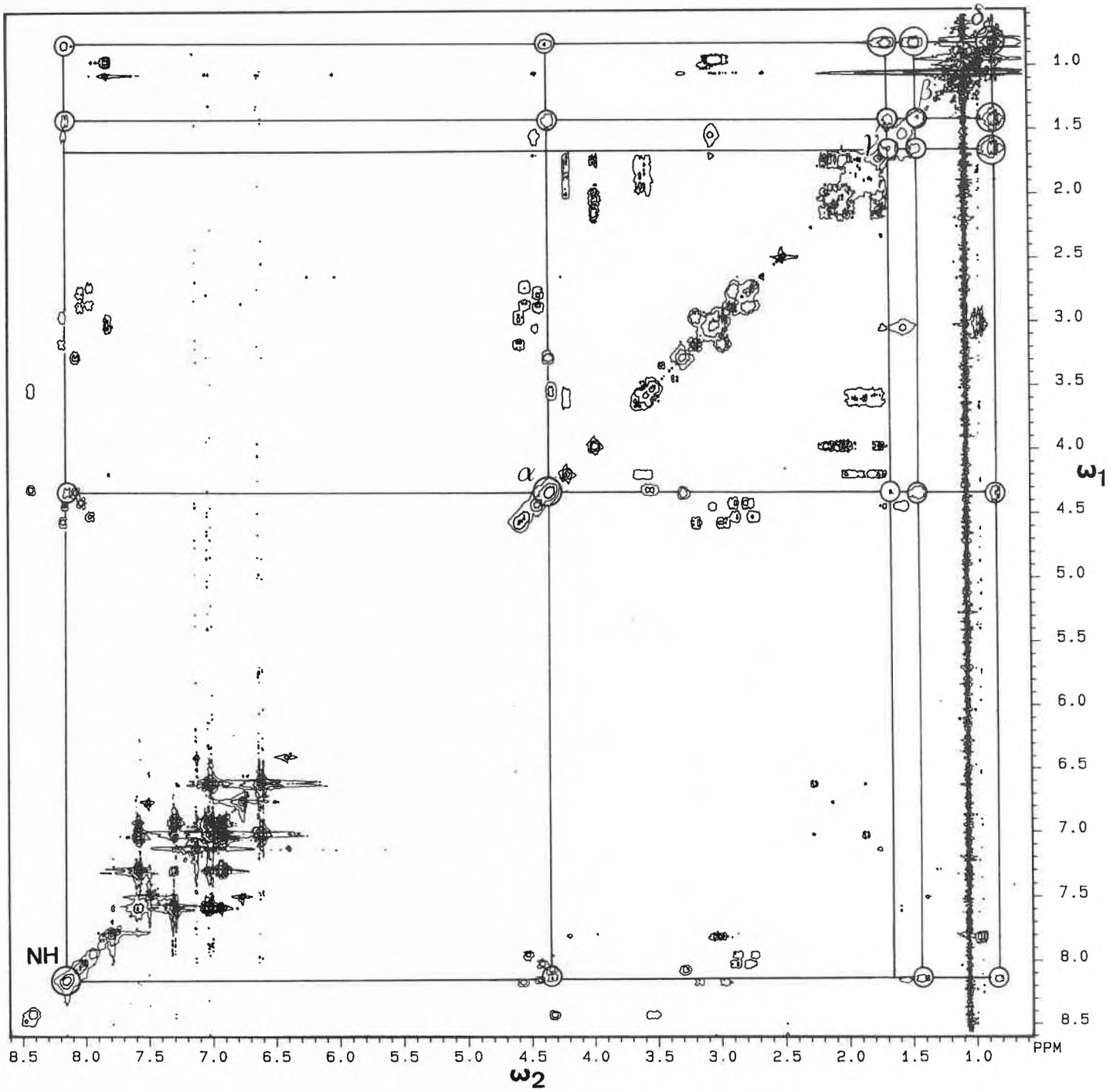

Fig. 15. 300 MHz TOCSY spectrum of the nonapeptide buserilin dissolved in dimethyl sulfoxide. The pulse sequence of Fig. 10d was applied with a mixing time $\tau_m = 112$ ms. The mixing process was effected by an MLEV-17 pulse sequence. A phase-sensitive plot with equal representation of positive and negative contours is shown. The resonance connectivities of leucine are indicated[19].

sign as a function of the rotational correlation time and can become very small. In the rotating frame, on the other hand, the cross-relaxation rate is always of the same sign and is larger than in the laboratory frame.

The cross-relaxation experiment in the rotating frame is called CAMELSPIN[23] or ROESY[24] and uses the same pulse sequence as TOCSY. In order to distinguish the origin of cross peaks it is possible to suppress TOCSY peaks by using their strong offset dependence[25] or by special pulse sequences[26].

9. Multiple Quantum Filtering

Among the experiments designed to simplify 2D correlation spectra, multiple quantum filtering plays a dominant role. Although it can also be applied to 1D spectra, it proved particularly useful in the context of 2D spectroscopy.

Multiple quantum coherence of order p can be understood as a coherent motion of p distinct spins in a molecule. It can be associated with a transition between two levels in the energy level diagram that differ in magnetic quantum number by ΔM = p. In other words, p spins change simultaneously their polarization in the course of a p-quantum transition. These transitions are so-called forbidden transitions in the sense that they cannot be observed directly. It is however possible to use an indirect detection scheme.

The basic idea of multiple quantum filtering is to eliminate from a spectrum the response of all those spin systems for which it is impossible to excite p-quantum coherence. Numerous cross peaks can be suppressed in this way based on the following principles[1, 27]:

(i) It is impossible to excite p-quantum coherence in spin systems with less than p coupled spins $I = ½$.

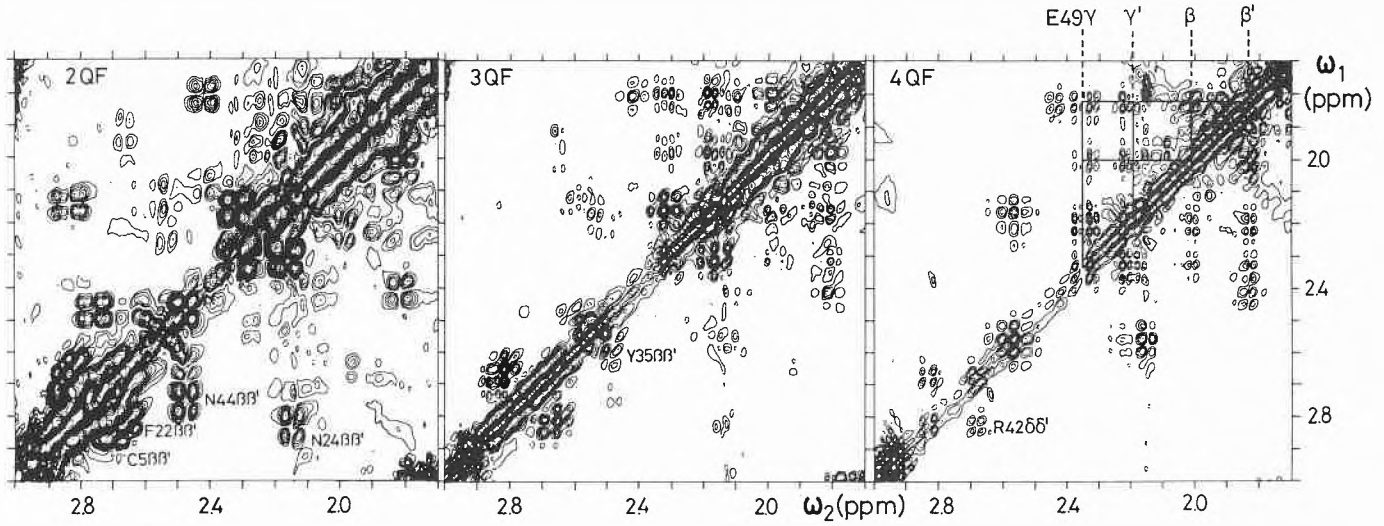

Fig. 16. Exerpts from 2-quantum, 3-quantum, and 4-quantum filtered COSY spectra of BPTI recorded at 360 MHz. The region shown contains primarily geminal cross peaks of aliphatic chains (reproduced from Ref. [29]*).*

(ii) For the appearance of the diagonal peak of spin I_k in a p-quantum filtered COSY spectrum, the spin I_k must be directly coupled to at least $p - 1$ further spins.

(iii) For the appearance of the cross peaks between spins I_k and I_l in a p-quantum filtered COSY spectrum, both spins must simultaneously be coupled to at least $p - 2$ further spins.

Violations of these coherence transfer selection rules occur for strong coupling and for certain special relaxation situations [28].

Fig. 16 shows excerpts from 2-, 3-, and 4-quantum filtered COSY spectra of BPTI in ^2H_2O. There is no restriction for the occurence of cross peaks in double quantum filtered COSY. However, in the 3- and 4-quantum filtered spectra many cross peaks are missing. The absence of the peaks C5$\beta\beta$', F22$\beta\beta$', N24$\beta\beta$', Y35$\beta\beta$', and N44$\beta\beta$' in the 4QF COSY spectrum follows already from rule (i) as the two β-protons form together with the single α-proton a three-spin system. That the peaks N24$\beta\beta$' and N44$\beta\beta$' are also absent in the 3QF COSY spectrum indicates that one of the couplings $C_\beta H$-$C_\alpha H$ or $C_\beta H'$-$C_\alpha H$ is very small and leads to peak suppression according to rule (iii). It is then possible to resolve the peak R42$\delta\delta$' in the 4QF spectrum which was hidden in the 2QF and 3QF spectra. In addition, also the region of the E49 cross peaks has become much clearer by 4-quantum filtering.

The principle of multiple quantum filtering relies on the selection of coherence transfer pathways as demonstrated by Fig. 17 [30]. The preparation pulse of the experiment excites coherence of order $p = \pm 1$ (precession of a single spin). In the course of the evolution period anti-phase coherence is established which can be transferred by the first mixing pulse into multiple quantum coherence of all allowed orders p (coherent precession of p spins). The allowance depends on the stated rules. At this moment a filtering operation is effected before the filtered coherence is made perceptible with the second mixing pulse by conversion into single quantum coherence.

The actual filtering operation is performed by a phase cycle of the first two pulses with the variable phase Φ indicated in Fig. 17. The phase of the multiple quantum coherence after the phase-shifted two-pulse excitation is proportional to its order p [31]

$$\Phi_p = p \cdot \Phi \qquad (7)$$

This can easily be understood by the involvement of p spins. Different orders experience therefore different phase shifts and can be separated by a suitable linear combination of results obtained by phase-shifted pulse sequences [31]. Double quantum filtering requires 4, 3-quantum filtering 6, and 4-quantum filtering 8 different phase-shifted experiments.

Another application of multiple quantum filtering is the famous INADEQUATE experiment, introduced by *Bax* et al. [32]. It allows the selection of those very rare molecules that carry two ^{13}C isotopes in natural abundance, and suppression of singly labeled molecules by double quantum filtering. The experiment is important for establishing connectivity of the carbon framework in medium-size molecules based on ^{13}C-^{13}C J couplings.

So far, multiple quantum transitions have been used just for filtration purposes. They are present only for a very brief period of a few microseconds between the second and third pulse in Fig. 17. On the other hand, it is also possible to take advantage of the evolution of multiple quantum coherence during the evolution

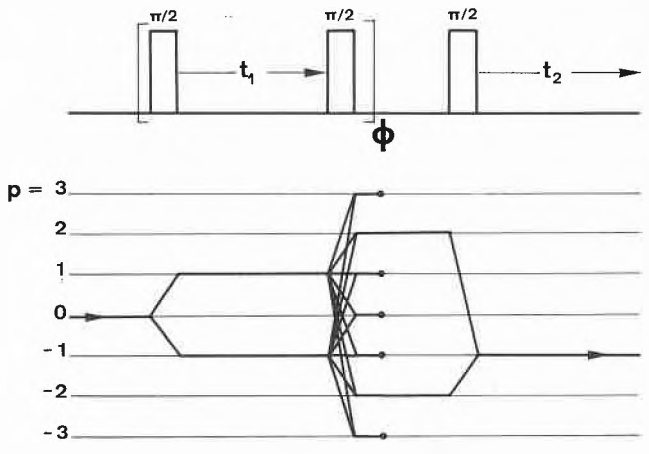

Fig. 17. Principle of multiple quantum filtering. The pulse sequence is shown together with a coherence level diagram in which each level designates coherence of a particular order p. Pulses cause a change of coherence order. The p-quantum filtering process (here p = 2) is performed by a phase cycle of the first two pulses, coadding the signals obtained for various phases Φ (here $\Phi = 0°, 90°, 180°, 270°$).

period. This leads to 2D multiple quantum spectroscopy[1, 33, 34] where multiple quantum transition frequencies along ω_1 are correlated with single quantum transition frequencies along ω_2. Multiple quantum frequencies are just the sum of the precession frequencies of all involved spins. The corresponding pulse scheme of Fig. 10e starts a multiple quantum excitation sequence consisting of two $\pi/2$ pulses and a central π chemical-shift-refocusing pulse. The single mixing pulse converts multiple quantum coherence into observable single quantum coherence.

2D multiple quantum spectroscopy reveals similar information as relayed correlation spectroscopy. It leads to cross peaks for direct and for remote connectivity, following simple rules[34]. Advantages are the absence of strong diagonal peaks and the simplicity of multiplets in the ω_1 direction. A practically important application is 2D INADEQUATE spectroscopy[35].

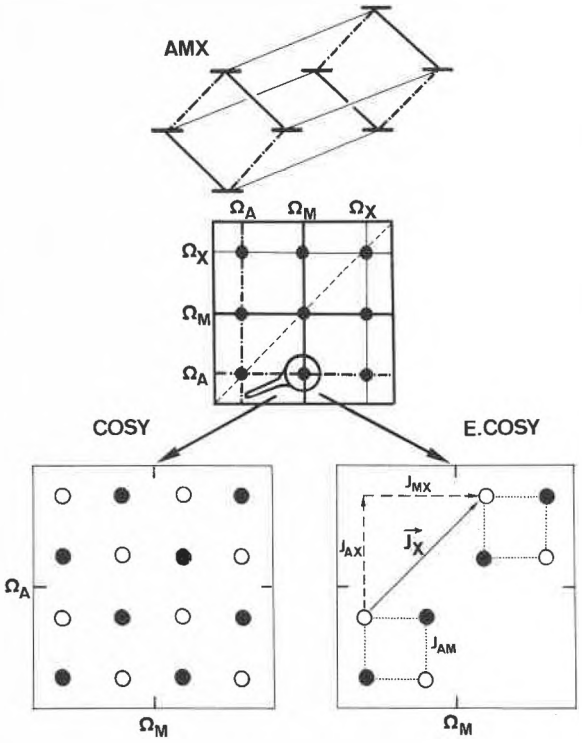

Fig. 18. Principle of exclusive correlation spectroscopy. At the top the energy level diagram of a three-spin system is given. A transitions: –·–·–, M transitions: ——, X transitions: ——. A cross peak from the full COSY spectrum in the center is enlarged at the bottom for COSY and for exclusive correlation spectroscopy. Positive intensities are shown by open circles, negative ones by filled circles.

10. Exclusive Correlation Spectroscopy

Exclusive correlation spectroscopy attempts to simplify cross-peak multiplet patterns by restricting coherence transfer to pairs of transitions that are connected in terms of the energy level diagram and share an energy level. This often enables a detailed analysis of the cross-peak multiplets in order to determine spin coupling constants that are useful for the structure determination of molecules.

Fig. 18 demonstrates the priniciples by means of an AMX three-spin system. The multiplet structure of the AM cross peak is shown at the lower left. It contains 16 multiplet components that correspond to coherence transfer between all four A and four M transitions. By restricting coherence transfer to connected transitions, only 8 multiplet components remain as shown at the lower right. The resulting multiplet structure can easily be understood. It consists of two basic squares with the side length equal to the «active» coupling J_{AM}. Each of the squares originates from an AM($\pm$½) spin system with spin X either in the m_X = ½ or –½ state. This corresponds to the transitions forming the perpendicular front or rear quadrilateral in the energy level diagram of Fig. 18. The relative displacement of the two squares in the 2D spectrum is determined by the two «passive» couplings J_{AX} and J_{MX}. Obviously, the determination of coupling constants is quite easy in an exclusive correlation spectrum, while COSY multiplets are often too complex for an analysis because of numerous overlaps.

The exclusive correlation cross peak $C_\gamma H_2$-$C_\delta H_1$ of proline[8] in the cyclic decapeptide antamanide, given in Fig. 19, demonstrates that also very small passive couplings can be determined by a comparison of horizontal cross sections cut through the

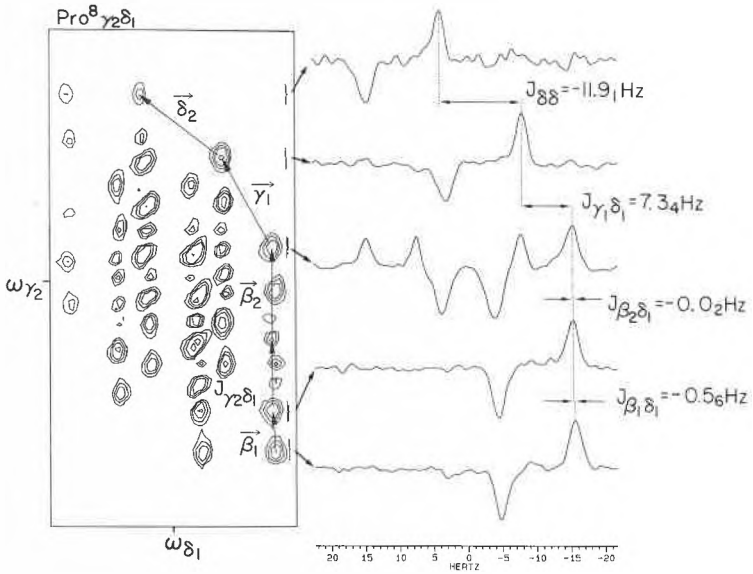

Fig. 19. $C_\gamma H_2$-$C_\delta H_1$ cross peak of proline[8] residue from a 300 MHz E. COSY spectrum of the cyclic decapeptide antamanide. In addition five horizontal cross sections are shown that have been obtained by vertical projection of the sections indicated by brackets. Displacement vectors by passive coupling constants are indicated in the contour plot. Passive coupling constants are determined by the horizontal displacement of cross sections (reproduced from Ref. [37]*).*

multiplet. Four displacement vectors corresponding to passive coupling pairs are indicated. It should be noted that the couplings can be much smaller than the width of the peaks when the spread in the orthogonal direction is sufficiently large to avoid overlap. In other words, only one of the two couplings from a passive spin to the two active ones must be resolved in order to allow the measurement of both.

Several experimental schemes have been proposed to obtain exclusive correlation spectra. The E. COSY technique employs a particular phase cycle, similar to multiple quantum filtering, in order to properly restrict coherence transfer[36, 37]. The β-COSY

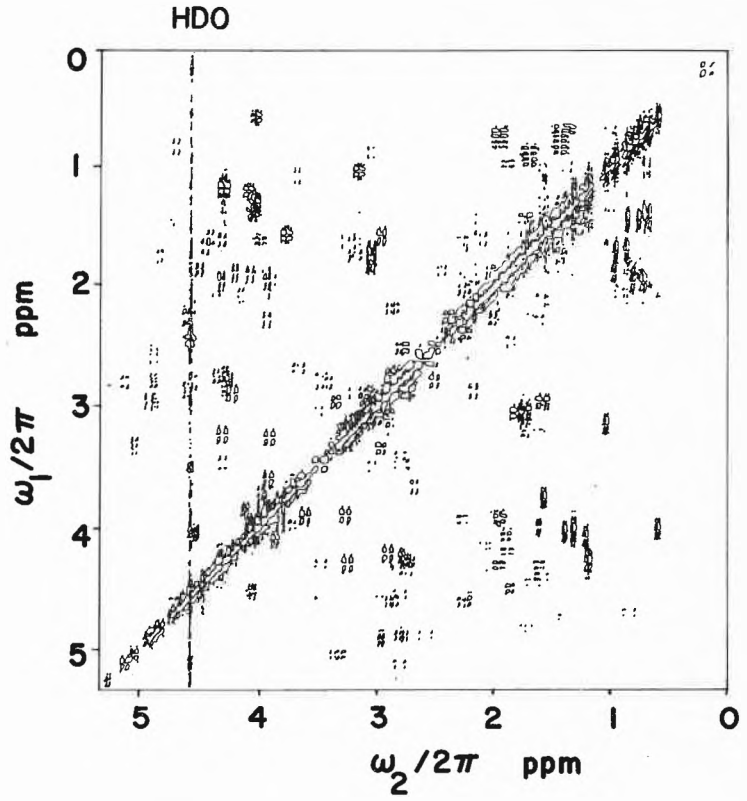

Fig. 20. Excerpt from a phase-sensitive double-quantum-filtered COSY spectrum of BPTI in ^2H_2O recorded at 300 MHz and 300 K (reproduced from Ref. [41]).

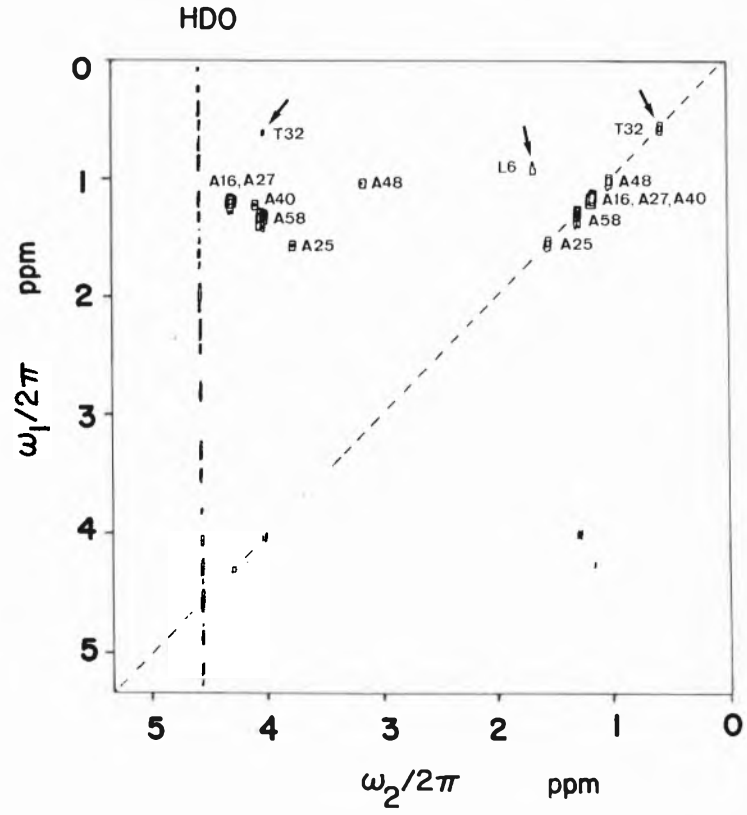

Fig. 21. Excerpt from an absolute value spin-topology-filtered COSY spectrum of BPTI in ^2H_2O recorded at 300 MHz and 300 K. The spin topology filter is optimized for the reception of the alanine spin system using the sequence shown in Fig. 22 (reproduced from Ref. [41]).

experiment[33, 38] that uses small rotation angles for the mixing pulse allows only approximate suppression of undesired multiplet components. Phase artefacts of the β-COSY experiment for strongly coupled spin systems can be eliminated by z-filtering, leading to z-COSY[39].

It should be noted that the same favourable multiplet structure is also produced in 2D correlation spectroscopy when using selective mixing pulses. This leads to the so-called soft-COSY technique[40].

11. Spin Topology Filtering

A further step in simplifying 2D spectra is filtering for specific topologies of the spin coupling network. In this way, it is possible to distinguish spin systems with the same number of spins but different spin-spin coupling topology. For example, four-spin systems can be linear, cyclic, or star-like in their coupling topology.

It has been shown that spin topology selection by adapted pulse sequences is possible in some cases[41]. The suppression of undesired spin systems is however often incomplete and depends not only on the coupling topology but also on the actual values of the coupling constants.

An example is shown in Figs. 20 and 21. The rather complex double-quantum-filtered COSY spectrum of BPTI in Fig. 20 can be simplified to the spectrum given in Fig. 21 by means of a pulse sequence that selects the four-spin coupling topology of alanine. The $C_\alpha H$ proton in alanine is coupled to each of the three equivalent $C_\beta H$ protons. The couplings among the $C_\beta H$ protons are ineffective, leading to a star-like coupling topology. The 2D spectrum of Fig. 21 is quite asymmetric due to the special pulse sequence used (Fig. 22). It is of the type of «constant time evolution»[38] that leads to ω_1-decoupled 2D spectra. All six alanine cross peaks are visible in the upper half of the 2D spectrum together with some «leakage» from threonine[32] and leucine[6] which contain similar groupings in their spin systems.

12. Computer Pattern Recognition

It has become apparent that 2D spectra are very rich in information content for large molecules, and their analysis can become quite demanding and time-consuming. The structure of 2D spectra follows well defined rules and it should therefore be possible to perform a spin-system analysis at least partially by a computer program with or without operator interaction.

Several attempts have been made in this direction[42–46]. It is possible to start with a detailed analysis, searching for the basic square patterns, mentioned in Section 10, and to build up successively cross peaks and coupling networks[42, 43]. On the other hand, it is also possible to employ cluster analysis procedures to localize cross peaks or cross-peak clusters which are then further analyzed by local symmetry analysis procedures[44, 45].

The recently developed local symmetry algorithm has been applied to the E.

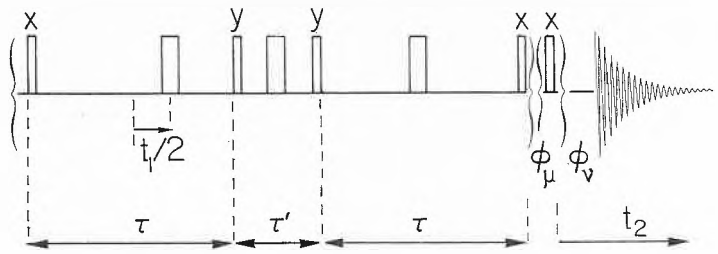

Fig. 22. Pulse sequence for AX_3 spin topology filtering. The sequence involves a constant time evolution period $2\tau + \tau'$ within which a π pulse is shifted as a function of the evolution time t_1. The phases Φ_μ and Φ_ν are varied to achieve four-quantum filtering (reproduced from Ref. [41]).

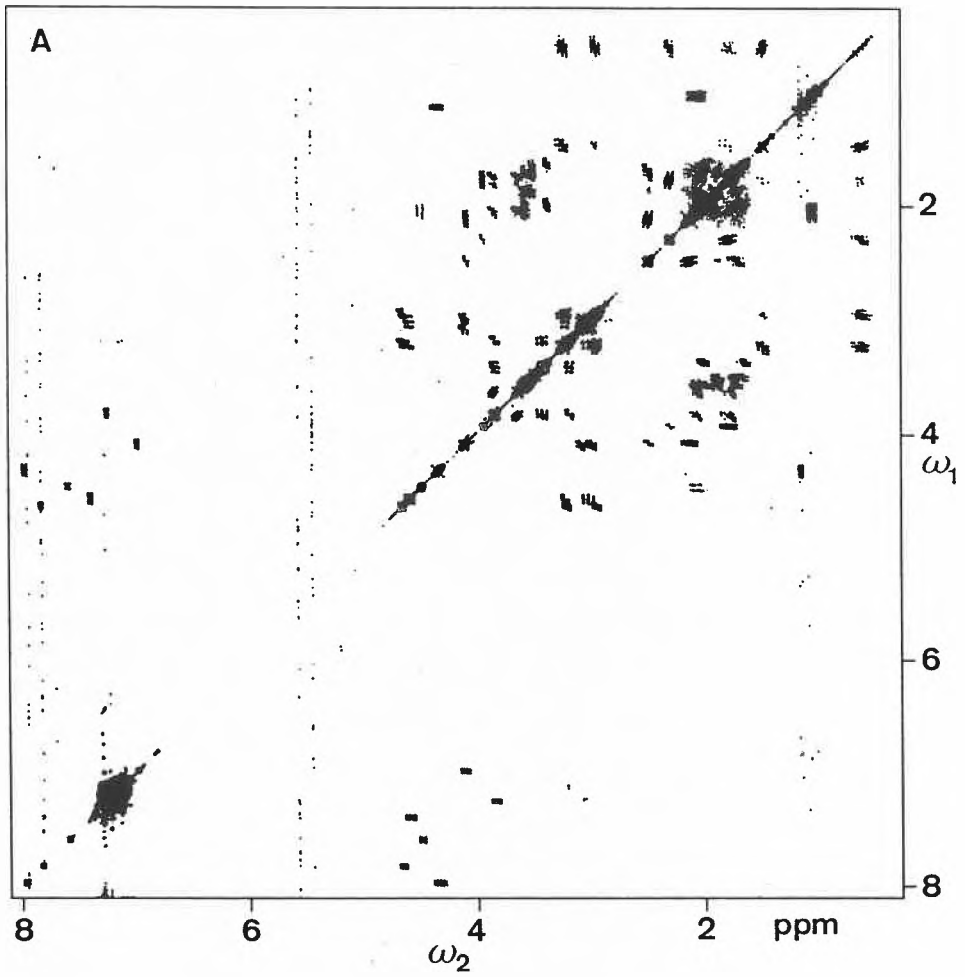

Fig. 23. 300 MHz proton resonance E.COSY spectrum of the cyclic decapeptide antamanide represented by a 2048 × 2048 data matrix. This spectrum was the input for the computer analysis that led to the connectivity diagram shown in Fig. 24 (reproduced from Ref. [45]).

COSY spectrum of the cyclic decapeptide antamanide, [-Val-Pro-Pro-Ala-Phe-Phe-Pro-Pro-Phe-Phe-], shown in Fig. 23[45]. At first cross peaks have been localized by a cluster analysis procedure[44]. The chemical shift centers together with some coupling constants have then been determined by a local symmetry analysis. By comparing shifts it was possible to deduce the connectivity diagram shown in Fig. 24. It represents eight of the ten spin systems of the molecule. Two strongly coupled spin systems of proline[2] and proline[7] could not been analyzed by this procedure. Here interactive fitting methods are required.

It appears at this moment that indeed much of the analysis of 2D spectra can be performed automatically, although a full analysis of a large protein or polynucleotide is not yet feasible.

13. Heteronuclear Correlation Spectroscopy

All experiments described so far are concerned with homonuclear spin systems using proton resonance. A great number of 2D experiments has also been developed for elucidating heteronuclear spin systems[1]. In fact, even more variants are conceivable in a heteronuclear environment where the different spin species can be perturbed by individual pulse sequences.

Of greatest practical importance is heteronuclear correlation spectroscopy[47, 48] where resonances of two different spin species are correlated. The most interesting pair of nuclei in this context is proton and carbon-13. The standard proton-carbon chemical shift correlation experiment starts with proton coherence excited by a proton $\pi/2$ pulse as shown in Fig. 25a. During the evolution time t_1, proton coherence is evolving. The following mixing process, consisting of $\pi/2$ pulses applied simultaneously to protons and carbons, transfers coherence to the carbon-13 spins. Their precession is observed during the detection period. The similarity to the homonuclear COSY experiment is evident.

Many variants are possible:

- (i) In order to allow ^{13}C decoupling during the evolution period, a refocusing π pulse is applied to ^{13}C in the center of the evolution period (Fig. 25b).
- (ii) Proton decoupling during detection can be effected by conventional heteronuclear decoupling (Fig. 25b).
- (iii) In order to allow for the formation of anti-phase coherence necessary for the coherence transfer despite of decoupling, fixed periods of evolution must be inserted before and after the mixing pulses (Fig. 25b).
- (iv) Sensitivity can be enhanced by interchanging evolution and detection periods, i.e. to start with ^{13}C evolution and use proton detection[47, 49].
- (v) To enhance the initial ^{13}C magnetization in variant (iv), polarization transfer from proton to ^{13}C is used.

It should be noted that predominantly cross peaks are observed between ^{13}C and directly attached protons due to the large one-bond couplings. The measurement of cross peaks to more remote protons with much weaker two- and three-bond couplings require further modifications of the basic pulse sequence[50].

Heteronuclear relayed coherence transfer experiments of the type $H \rightarrow H \rightarrow {}^{13}C$ (Fig. 25c) are quite useful to establish connectivity of >CH–, $-CH_2-$, and $-CH_3$ fragments[51, 52]. They provide a competitive and more sensitive alternative to INADEQUATE experiments.

An experimental example of a heteronuclear relay experiment for the hexapeptide *cyclo*-[Phe[7]-Trp-Lys(Z)-Thr-Phe[11]-Pro] is given in Fig. 26[52]. The 2D shift correlation spectrum shows the direct connectivity peaks filled in black and labeled with the one-letter codes for the amino acid segments. In addition, numerous relayed cor-

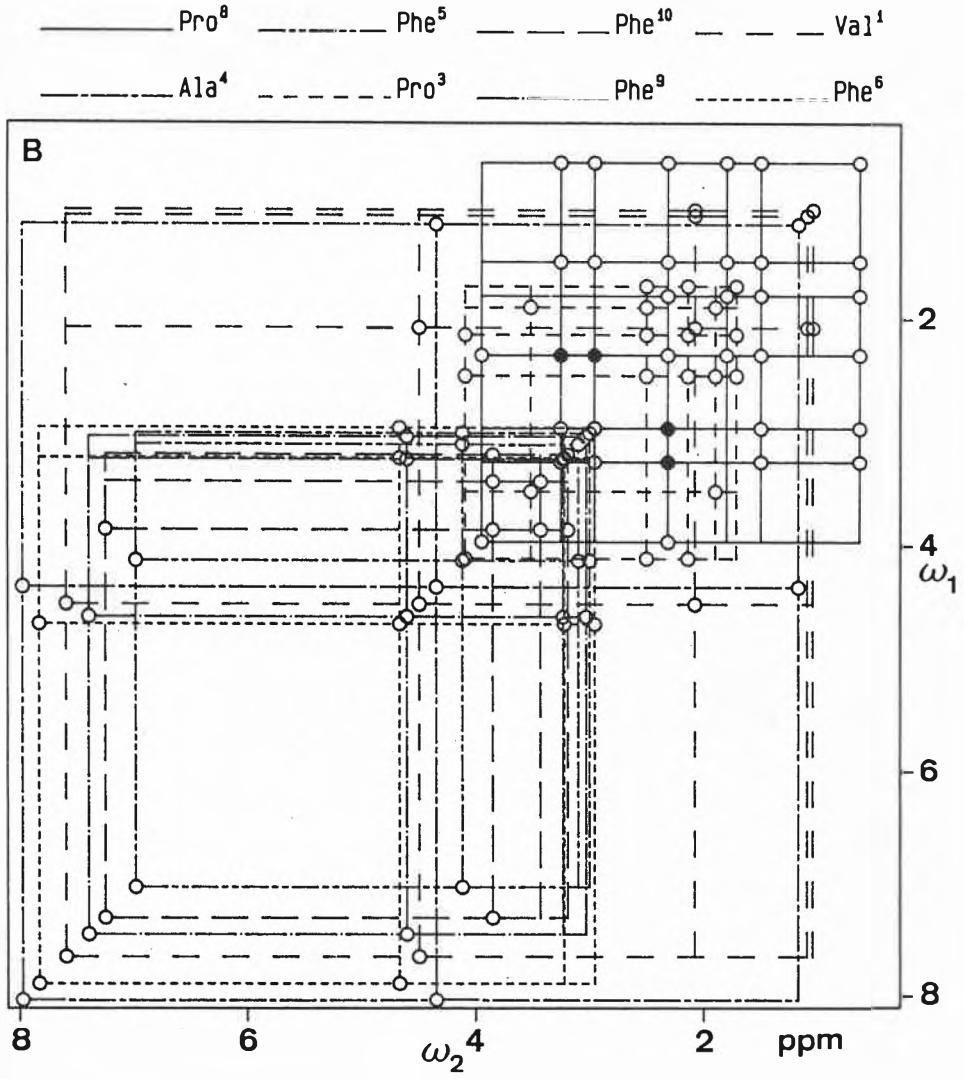

Fig. 24. Computer-generated connectivity diagram of the eight recognized spin systems Pro⁸, Ala⁴, Phe⁵, Pro³, Phe¹⁰, Phe⁹, Val¹, and Phe⁶ of antamanide deduced from the experimental spectrum of Fig. 23 (reproduced from Ref. [45]).

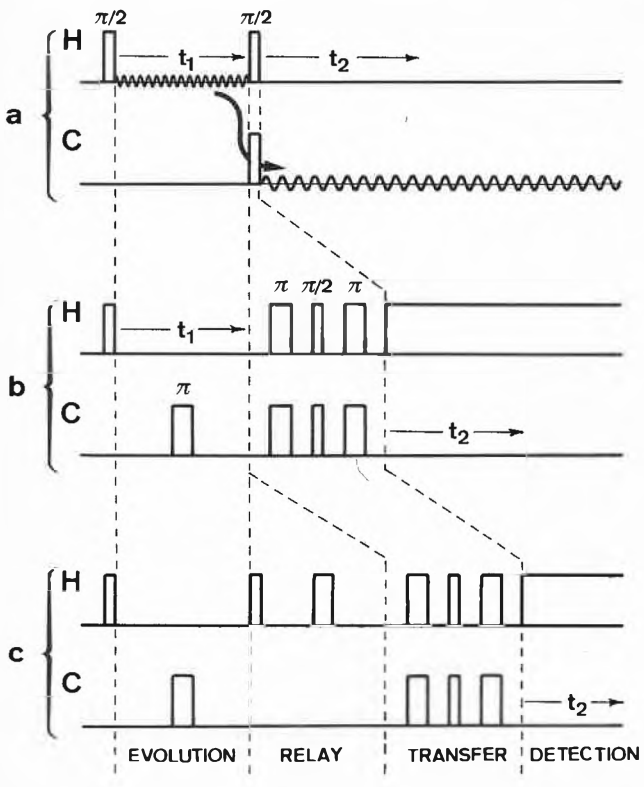

Fig. 25. Pulse sequences for heteronuclear correlation spectroscopy. – (a) Standard sequence with two simultaneous mixing pulses applied to proton and carbon spins in order to transfer coherence from proton to carbon. – (b) Modified sequence allowing for ^{13}C spin decoupling (by π refocusing pulse) during evolution and ^{1}H spin decoupling (by continuous wave or multiple pulse irradation) during detection. – (c) Pulse sequence for heteronuclear relayed correlation spectroscopy with the transfers $H \rightarrow H \rightarrow {}^{13}C$.

relation peaks are visible that allow an easy assignment. Connectivities are indicated for threonine and for lysine.

Properly assigned ^{13}C resonances in biomolecules are of importance for the determination of local mobility through a measurement of ^{13}C T_1's. This possibility is based on the dominant influence on relaxation of the directly bounded protons whose distances from the ^{13}C nuclei are accurately known. The relaxation time T_1 can then be related directly to a correlation time τ_c characterizing mobility.

14. Conclusions and Outlook

The realm of 2D spectroscopy is almost unlimited. A new dimension has not only been introduced into the spectrum but also in the experimental design resulting in a large multitude of novel techniques, many of them with interesting practical applications. This essay has provided a rather limited account of these techniques. Many sizeable classes of methods have been fully ignored. For a more detailed account of two-dimensional spectroscopy and the underlying principles, the reader is referred to the recent monograph [1].

Although most of the information contained in 2D spectra can also be obtained by careful one-dimensional experiments, 2D spectroscopy is the method of choice in many situations. In particular for obtaining a survey on the properties of a molecular system, 2D spectroscopy is unbeatable. To perform a 2D experiment requires only minimum previous knowledge on the system to be investigate, and the danger to overlook unexpected but important facts is minimized. Obviously for obtaining an answer to a very specific question on a limited aspect of a molecule, it might still be easier and faster to perform a specific one-dimensional experiment. But very often all relevant specific questions can be answered based on a single two-dimensional experiment.

It is likely that in the future 2D NMR spectroscopy will become one of the most powerful tools in particular for the molecular biologist. Not only structure but hopefully also dynamics of medium to large size biomolecules in solution can be determined by this technique. In this re-

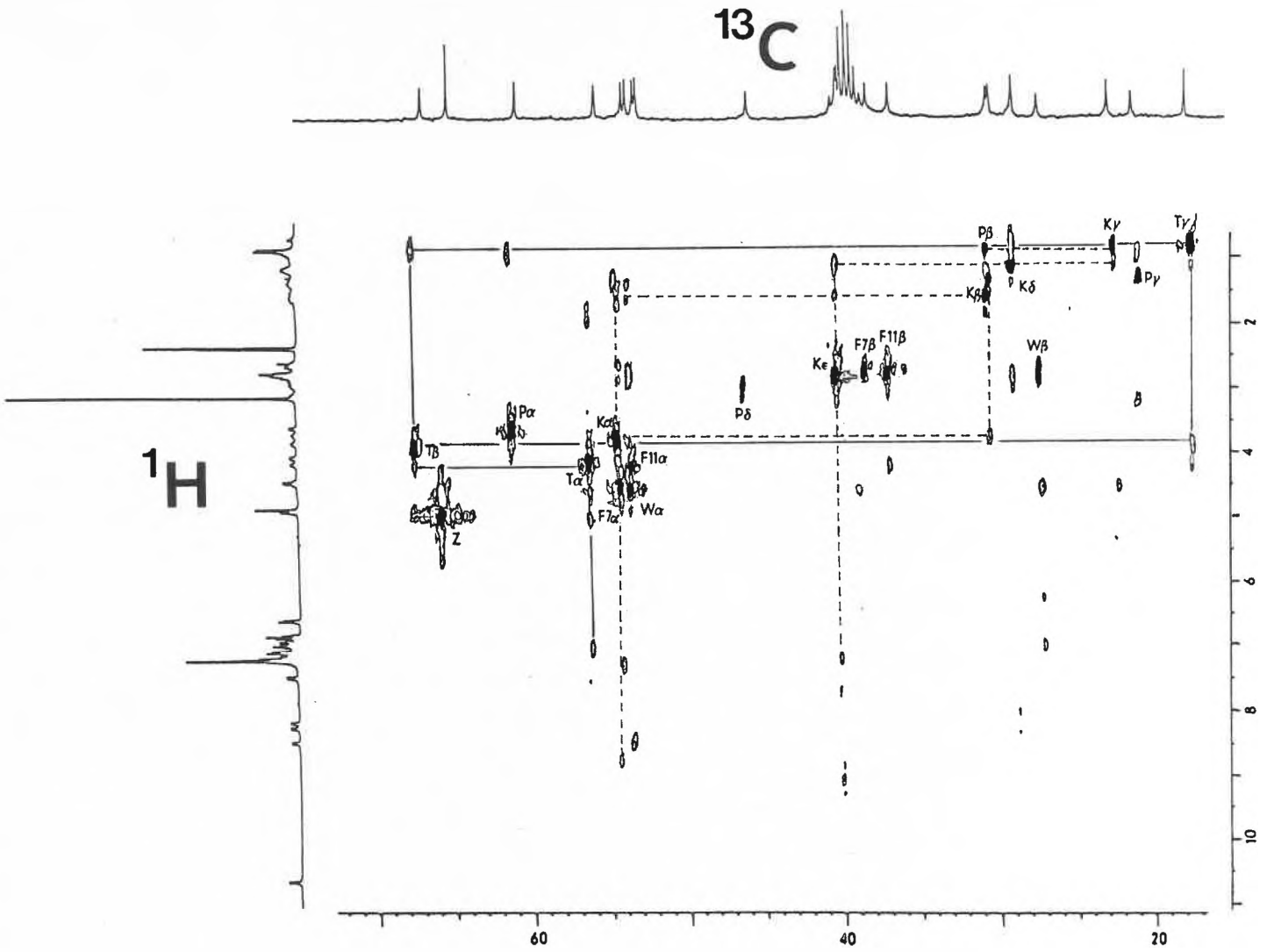

Fig. 26. Relayed 300 MHz ^1H-^{13}C shift correlation spectrum of cyclo-[Phe^7-Trp-Lys(Z)-Thr-Phe^{11}-Pro]. A pulse sequence equivalent to Fig. 25c was used. The full ^1H spectrum is correlated with the aliphatic region of the ^{13}C spectrum. The direct connectivity peaks that are also visible in a standard correlation spectrum are filled in black and labeled with one-letter codes. The remaining peaks are relayed correlation peaks. The connectivities of neighbouring >CH–, –CH$_2$–, and –CH$_3$ fragments are indicated for threonine (full lines) and lysine (broken lines) (adapted from Ref. [52]*).*

spect, the method is truely unique. In view of further developments of instrumentation and computer procedures, 2D spectroscopy has the potential of becoming a routine technique that may lead to almost fully automated determination of molecular structure.

Perhaps as important as the practical application of 2D spectroscopy are the conceptual aspects of the new approach. It has provided impetus to entire NMR technology. Numerous new techniques have emerged that have on the first sight no direct connection to 2D spectroscopy. To mention a few techniques, heteronuclear polarization transfer by methods such as INEPT[53] and DEPT[54] is a descendent of 2D spectroscopy that is indispensible for sensitivity enhancement and spectral editing. Methods for indirect detection of resonance can be considered as 2D techniques with one-dimensional Fourier transformation. In this context, multiple quantum spectroscopy[55] and zero field magnetic resonance with field cycling[56] should be mentioned.

What has initially appeared to be just a curiosity that produced intriguing and aesthetically pleasing plots became a powerful tool with a vast number of applications in fields of science ranging from solid state physics, through chemistry and biology to medicine. Further developments are to be expected in this field.

Incidentally, I would like to mention that the very first paper that has ever been published on 2D spectroscopy appeared in *Chimia* in 1975[57]. A comparison with the present paper reveals the enormous progress that has been made since 1975.

Acknowledgements: The author acknowledges the creative contributions of a great number of co-workers during the past 13 years of activity in two-dimensional spectroscopy. They all are co-authors on one or more of the cited papers. Particular gratitude is owed to Professor Kurt Wüthrich and his co-workers for a very fruitful collaboration in the development of 2D techniques relevant for biological applications. The buserilin spectra shown in Figs. 13–15 were kindly supplied by Dr. Christian Griesinger[19]*. The projects have been supported by the Swiss National Science Foundation, the Kommission zur Förderung der wissenschaftlichen Forschung, and Spectrospin AG, Fällanden. The manuscript has been processed by Mrs. Marianne Bösch.*

Received: August 12, 1987 [FR42]

[1] R. R. Ernst, G. Bodenhausen, A. Wokaun: *Principles of Nuclear Magnetic Resonance in One and Two Dimensions*, Clarendon Press, Oxford (1987).
[2] K. Wüthrich: *NMR of Proteins and Nucleic Acids*, Wiley-Interscience, New York (1986).
[3] Chandrakumar, S. Subramanian: *Modern Techniques in High-Resolution FT-NMR*, Springer, Berlin (1987).

[4] P.G. Morris: *Nuclear Magnetic Resonance Imaging in Medicine and Biology*, Clarendon Press, Oxford (1986).
[5] M. Saunders, in A. Ehrenberg, B.G. Malmström, T. Vänngård (Ed.): *Magnetic Resonance in Biological Systems*, Pergamon Press, Oxford (1967), p. 85.
[6] B.H. Meier, R.R. Ernst, *J. Am. Chem. Soc. 101* (1979) 6441.
[7] T.F. Havel, K. Wüthrich, *Bull. Math. Biol. 46* (1984) 673; *J. Mol. Biol. 182* (1985) 281.
[8] R. Kaptein, E.R.P. Zuiderweg, R.M. Scheek, R. Boelens, W.F. Gundsteren, *J. Mol. Biol. 182* (1985) 179; G.M. Clore, A.M. Gronenborn, A.T. Brünger, M. Karplus, *ibid. 186* (1985) 435.
[9] Anil Kumar, R.R. Ernst, K. Wüthrich, *Biochem. Biophys. Res. Commun. 95* (1980) 1.
[10] G. Wagner, Anil Kumar, K. Wüthrich, *Eur. J. Biochem. 114* (1981) 375.
[11] M.P. Williamson, T.F. Havel, K. Wüthrich, *J. Mol. Biol. 182* (1985) 295.
[12] P. Caravatti, P. Neuenschwander, R.R. Ernst, *Macromolecules 19* (1986) 1889.
[13] P. Caravatti, P. Neuenschwander, R.R. Ernst, *Macromolecules 18* (1985) 119.
[14] B. Blümich, *Prog. NMR Spectrosc. 19* (1987) 331.
[15] O.W. Sørensen, G.W. Eich, M.H. Levitt, G. Bodenhausen, R.R. Ernst, *Prog. NMR Spectrosc. 16* (1983) 163.
[16] J. Jeener, Ampere Int. Summer School II, Basko Polje, Yugoslavia (1971).
[17] Anil Kumar, D. Welti, R.R. Ernst, *J. Magn. Reson. 18* (1975) 69.
[18] G.W. Eich, G. Bodenhausen, R.R. Ernst, *J. Am. Chem. Soc. 104* (1982) 3731.
[19] C. Griesinger, unpublished work (1987).
[20] L. Braunschweiler, R.R. Ernst, *J. Magn. Reson. 53* (1983) 521.
[21] A. Bax, D.G. Davis, *J. Magn. Reson. 65* (1985) 355.
[22] S.R. Hartmann, E.C. Hahn, *Phys. Rev. 128* (1962) 2042.
[23] A.A. Bothner-By, R.L. Stephens, J. Lee, C.D. Warren, R.W. Jeanloz, *J. Am. Chem. Soc. 106* (1984) 811.
[24] A. Bax, D.G. Davis, *J. Magn. Reson. 63* (1985) 207.
[25] C. Griesinger, R.R. Ernst, *J. Magn. Reson.*, in press.
[26] H. Kessler, C. Griesinger, R. Kressebaum, K. Wagner, R.R. Ernst, *J. Am. Chem. Soc. 109* (1987) 607.
[27] U. Piantini, O.W. Sørensen, R.R. Ernst, *J. Am. Chem. Soc. 104* (1982) 6800.
[28] N. Müller, G. Bodenhausen, K. Wüthrich, R.R. Ernst, *J. Magn. Reson. 65* (1985) 531.
[29] N. Müller, R.R. Ernst, K. Wüthrich, *J. Am. Chem. Soc. 108* (1986) 6482.
[30] G. Bodenhausen, H. Kogler, R.R. Ernst, *J. Magn. Reson. 58* (1984) 370.
[31] A. Wokaun, R.R. Ernst, *Chem. Phys. Lett. 52* (1977) 407.
[32] A. Bax, R. Freeman, S.P. Kempsell, *J. Am. Chem. Soc. 102* (1980) 4849.
[33] W.P. Aue, E. Bartholdi, R.R. Ernst, *J. Chem. Phys.* 64 (1976) 2229.
[34] L. Braunschweiler, G. Bodenhausen, R.R. Ernst, *Mol. Phys. 48* (1983) 535.
[35] T.H. Mareci, R. Freeman, *J. Magn. Reson. 48* (1982) 158.
[36] C. Griesinger, O.W. Sørensen, R.R. Ernst, *J. Am. Chem. Soc. 107* (1985) 6394.
[37] C. Griesinger, O.W. Sørensen, R.R. Ernst, *J. Chem. Phys. 85* (1986) 6837.
[38] A. Bax, R. Freeman, *J. Magn. Reson. 44* (1981) 542.
[39] H. Oschkinat, A. Pastore, P. Pfändler, G. Bodenhausen, *J. Magn. Reson. 69* (1986) 559.
[40] J.R. Brüschweiler, J.C. Madsen, C. Griesinger, O.W. Sørensen, R.R. Ernst, *J. Magn. Reson. 73* (1987) 380.
[41] M.H. Levitt, R.R. Ernst, *J. Chem. Phys. 83* (1985) 3297.
[42] B.U. Meier, G. Bodenhausen, R.R. Ernst, *J. Magn. Reson. 60* (1984) 161.
[43] P. Pfändler, G. Bodenhausen, B.U. Meier, R.R. Ernst, *Anal. Chem. 57* (1985) 2510.
[44] Z. Mádi, B.U. Meier, R.R. Ernst, *J. Magn. Reson. 72* (1987) 584.
[45] B.U. Meier, Z. Mádi, R.R. Ernst, *J. Magn. Reson.*, in press.
[46] P. Pfändler, G. Bodenhausen, *J. Magn. Reson. 70* (1986) 71; M. Novič, H. Oschkinat, P. Pfändler, G. Bodenhausen, *ibid. 73* (1987) 493.
[47] A.A. Maudsley, R.R. Ernst, *Chem. Phys. Lett. 50* (1977) 368; A.A. Maudsley, L. Müller, R.R. Ernst, *J. Magn. Reson. 28* (1977) 463.
[48] G. Bodenhausen, R. Freeman, *J. Magn. Reson. 28* (1977) 471.
[49] D.H. Live, D.G. Davis, W.C. Agosta, D. Cowburn, *J. Am. Chem. Soc. 106* (1984) 6104.
[50] S. Wimperis, R. Freeman, *J. Magn. Reson. 58* (1984) 348.
[51] P.H. Bolton, G. Bodenhausen, *Chem. Phys. Lett. 89* (1982) 139.
[52] H. Kessler, M. Bernd, H. Kogler, Z. Zarbock, O.W. Sørensen, G. Bodenhausen, R.R. Ernst, *J. Am. Chem. Soc. 105* (1983) 6944.
[53] G.A. Morris, R. Freeman, *J. Am. Chem. Soc. 101* (1979) 760; D.P. Burum, R.R. Ernst, *J. Magn. Reson. 39* (1980) 163.
[54] D.M. Doddrell, D.T. Pegg, M.R. Bendall, *J. Magn. Reson. 48* (1982) 323.
[55] G. Bodenhausen, *Prog., NMR Spectrosc. 14* (1981) 137; D.P. Weitekamp, *Adv. Magn. Reson. 11* (1983) 111.
[56] D.P. Weitekamp, A. Bielecki, D.B. Zax, K.W. Zilm, A. Pines, *Phys. Rev. Lett. 50* (1983) 1807; A. Bielecki, J.B. Murdoch, D.P. Weitekamp, D.B. Zax, K.W. Zilm, H. Zimmermann, A. Pines, *J. Chem. Phys. 80* (1984) 2232.
[57] R.R. Ernst, *Chimia 29* (1975) 179.